Heavy SUSY Higgs Bosons at e^+e^- Linear Colliders

A. Djouadi[1,2], J. Kalinowski[3], P. Ohmann[1,4] and P.M. Zerwas[1]

[1] Deutsches Elektronen–Synchrotron DESY, D-22603 Hamburg, FRG.

[2] Institut für Theoretische Physik, Universität Karlsruhe, D-76128 Karlsruhe, FRG.

[3] Institute of Theoretical Physics, Warsaw University, PL-00681 Warsaw, Poland.

[4] Department of Theoretical Physics, Oxford University, OX1 3NP, Oxford, UK.

Abstract

The production mechanisms and decay modes of the heavy neutral and charged Higgs bosons in the Minimal Supersymmetric Standard Model are investigated at future e^+e^- colliders in the TeV energy regime. We generate supersymmetric particle spectra by requiring the MSSM Higgs potential to produce correct radiative electroweak symmetry breaking, and we assume a common scalar mass m_0, gaugino mass $m_{1/2}$ and trilinear coupling A, as well as gauge and Yukawa coupling unification at the Grand Unification scale. Particular emphasis is put on the low $\tan\beta$ solution in this scenario where decays of the Higgs bosons to Standard Model particles compete with decays to supersymmetric charginos/neutralinos as well as sfermions. In the high $\tan\beta$ case, the supersymmetric spectrum is either too heavy or the supersymmetric decay modes are suppressed, since the Higgs bosons decay almost exclusively into b and τ pairs. The main production mechanisms for the heavy Higgs particles are the associated AH production and H^+H^- pair production with cross sections of the order of a few fb.

1. Introduction

Supersymmetric theories [1, 2] are generally considered to be the most natural extensions of the Standard Model (SM). This proposition is based on several points. In these theories, fundamental scalar Higgs bosons [3, 4] with low masses can be retained in the context of high unification scales. Moreover, the prediction [5] of the renormalized electroweak mixing angle $\sin^2\theta_W = 0.2336 \pm 0.0017$, based on the spectrum of the Minimal Supersymmetric Standard Model (MSSM) [6], is in striking agreement with the electroweak precision data which yield $\sin^2\theta_W = 0.2314(3)$ [7]. An additional attractive feature is provided by the opportunity to generate the electroweak symmetry breaking radiatively [8]. If the top quark mass is in the range between ~ 150 and ~ 200 GeV, the universal squared Higgs mass parameter at the unification scale decreases with decreasing energy and becomes negative at the electroweak scale, thereby breaking the $\mathrm{SU(2)_L \times U(1)_Y}$ gauge symmetry while leaving the U(1) electromagnetic and SU(3) color gauge symmetries intact [8]. The analysis of the electroweak data prefers a light Higgs mass [7, 9] as predicted in supersymmetric theories; however since the radiative corrections depend only logarithmically on the Higgs mass [10], the dependence is weak and no firm conclusions can yet be drawn.

The more than doubling the spectrum of states in the MSSM gives rise to a rather large proliferation of parameters. This number of parameters is however reduced drastically by embedding the low–energy supersymmetric theory into a grand unified (GUT) framework. This can be achieved in supergravity models [8], in which the effective low–energy supersymmetric theory [including the interactions which break supersymmetry] is described by the following parameters: the common scalar mass m_0, the common gaugino mass $m_{1/2}$, the trilinear coupling A, the bilinear coupling B, and the Higgs–higgsino mass parameter μ. In addition, two parameters are needed to describe the Higgs sector: one Higgs mass parameter [in general the mass of the pseudoscalar Higgs boson, M_A] and the ratio of the vacuum expectation values, $\tan\beta = v_2/v_1$, of the two Higgs doublet fields which break the electroweak symmetry.

The number of parameters can be further reduced by introducing additional constraints which are based on physically rather natural assumptions:

(*i*) Unification of the b and τ Yukawa couplings at the GUT scale [11] leads to a correlation between the top quark mass and $\tan\beta$ [12, 13, 14]. Adopting the central value of the top mass as measured at the Tevatron [15], $\tan\beta$ is restricted to two narrow ranges around $\tan\beta \sim 1.7$ and $\tan\beta \sim 50$, with the low $\tan\beta$ solution theoretically somewhat favored [14].

(*ii*) If the electroweak symmetry is broken radiatively, then the bilinear coupling B and the Higgs–higgsino mass parameter μ are determined up to the sign of μ. [The sign of μ might be determined by future precision measurements of the radiative b decay amplitude.]

(*iii*) It turns out *a posteriori* that the physical observables are nearly independent of the GUT scale value of the trilinear coupling A_G, for $|A_G| \lesssim 500$ GeV.

Mass spectra and couplings of all supersymmetric particles and Higgs bosons are determined after these steps by just two mass parameters along with the sign of μ; we shall choose to express our results in terms of the pseudoscalar Higgs boson A mass M_A and the common GUT gaugino mass $m_{1/2}$.

In this paper we focus on heavy Higgs particles A, H and $H^\pm$ with masses of a few hundred GeV, and therefore close to the decoupling limit [16]. The pattern of Higgs masses is quite regular in this limit. While the upper limit on the mass of the lightest CP–even Higgs boson h is a function of $\tan\beta$ [17],

$$M_h \lesssim 100 \text{ to } 150 \text{ GeV} \quad [\text{for low to high } \tan\beta] \tag{1.1}$$

the heavy Higgs bosons are nearly mass degenerate [c.f. Fig.1]

$$M_A \simeq M_H \simeq M_{H^\pm} \tag{1.2}$$

Moreover, the properties of the lightest CP–even Higgs boson h become SM–like in this limit. The production of the heavy Higgs bosons becomes particularly simple in e^+e^- collisions; the heavy Higgs bosons can only be pair–produced,

$$\begin{aligned} e^+e^- &\to A\,H \qquad (1.3)\\ e^+e^- &\to H^+H^- \qquad (1.4)\end{aligned}$$

Close to this decoupling limit, the cross section for H Higgs–strahlung $e^+e^- \to ZH$ is very small and the cross section for the WW fusion mechanism $e^+e^- \to \nu_e\bar{\nu}_e H$ is appreciable only for small values of $\tan\beta$, $\tan\beta \sim 1$, and relatively small H masses, $M_H \lesssim 350$ GeV. The cross section for ZZ fusion of the H is suppressed by an order of magnitude compared to WW fusion. The pseudoscalar A particle does not couple to W/Z boson pairs at the tree level.

The decay pattern for heavy Higgs bosons is rather complicated in general. For large $\tan\beta$ the SM fermion decays prevail. For small $\tan\beta$ this is true above the $t\bar{t}$ threshold of $M_{H,A} \gtrsim 350$ GeV for the neutral Higgs bosons and above the $t\bar{b}$ threshold of $M_{H^\pm} \gtrsim 180$ GeV for the charged Higgs particles. Below these mass values many decay channels compete with each other: decays to SM fermions $f\bar{f}$ [and for H to gauge bosons VV], Higgs cascade decays, chargino/neutralino $\chi_i\chi_j$ decays and decays to supersymmetric sfermions $\tilde{f}\bar{\tilde{f}}$

$$\begin{aligned} H &\to f\bar{f}\ ,\ VV\ ,\ hh\ ,\ \chi_i\chi_j\ ,\ \tilde{f}\bar{\tilde{f}} \qquad (1.5)\\ A &\to f\bar{f}\ ,\ hZ\ ,\ \chi_i\chi_j\ ,\ \tilde{f}\bar{\tilde{f}} \qquad (1.6)\\ H^\pm &\to f\bar{f}'\ ,\ hW^\pm\ ,\ \chi_i\chi_j\ ,\ \tilde{f}\bar{\tilde{f}}\,' \qquad (1.7)\end{aligned}$$

In this paper, we analyze in detail the decay modes of the heavy Higgs particles and their production at e^+e^- linear colliders. The analysis will focus on heavy particles for which machines in the TeV energy range are needed. The paper is organized in the following way. In the next section we define the physical set–up of our analysis in the framework of the MSSM embedded into a minimal supergravity theory. In section 3, we discuss the production cross sections of the heavy Higgs bosons. In the subsequent sections, we discuss the widths of the various decay channels and the final Higgs decay products.

2. The Physical Set–Up

The Higgs sector of the Minimal Supersymmetric Standard Model is described at tree-level by the following potential

$$\begin{aligned} V_0 &= (m_{H_1}^2+\mu^2)|H_1|^2 + (m_{H_2}^2+\mu^2)|H_2|^2 - m_3^2(\epsilon_{ij}{H_1}^i{H_2}^j + \text{h.c.})\\ &\quad +\frac{1}{8}(g^2+g'^2)\left[|H_1|^2-|H_2|^2\right]^2 + \frac{1}{2}g^2|H_1^{i*}H_2^i|^2 \qquad (2.1)\end{aligned}$$

The quadratic Higgs terms associated with μ and the quartic Higgs terms coming with the electroweak gauge couplings g and g' are invariant under supersymmetric transformations. m_{H_1}, m_{H_2} and m_3 are soft–supersymmetry breaking parameters with $m_3^2 = B\mu$. ϵ_{ij} $[i,j = 1,2$ and $\epsilon_{12} = 1]$ is the antisymmetric tensor in two dimensions and $H_1 \equiv (H_1^1, H_1^2) = (H_1^0, H_1^-)$, $H_2 \equiv (H_2^1, H_2^2) = (H_2^+, H_2^0)$ are the two Higgs-doublet fields. After the symmetry breaking, three out of the initially eight degrees of freedom will be absorbed to generate the $W^\pm$ and Z masses, leaving a quintet of scalar Higgs particles: two CP–even Higgs bosons h and H, a CP–odd [pseudoscalar] boson A and two charged Higgs particles $H^\pm$.

Retaining only the [leading] Yukawa couplings of the third generation

$$\lambda_t = \frac{\sqrt{2}m_t}{v \sin\beta}\ , \quad \lambda_b = \frac{\sqrt{2}m_b}{v \cos\beta} \quad \text{and} \quad \lambda_\tau = \frac{\sqrt{2}m_\tau}{v \cos\beta} \tag{2.2}$$

where $\tan\beta = v_2/v_1$ [with $v^2 = v_1^2 + v_2^2$ fixed by the W mass, $v = 246$ GeV] is the ratio of the vacuum expectation values of the fields H_2^0 and H_1^0, the superpotential is given in terms of the superfields $Q = (t,b)$ and $L = (\tau, \nu_\tau)$ by[1]

$$W = \epsilon_{ij}\left[\lambda_t H_2^i Q^j t^c + \lambda_b H_1^i Q^j b^c + \lambda_\tau H_1^i L^j \tau^c - \mu H_1^i H_2^j\right] \tag{2.3}$$

Supersymmetry is broken by introducing the soft–supersymmetry breaking bino $\tilde{B}$, wino $\tilde{W}^a$ [a =1–3] and gluino $\tilde{g}^a$ [a =1–8] mass terms,

$$\frac{1}{2} M_1 \overline{\tilde{B}}\, \tilde{B} \ + \ \frac{1}{2} M_2 \overline{\tilde{W}}^a\, \tilde{W}^a \ + \ \frac{1}{2} M_3 \overline{\tilde{g}}^a\, \tilde{g}^a\ , \tag{2.4}$$

soft–supersymmetry breaking trilinear couplings,

$$\epsilon_{ij}\left[\lambda_t A_t H_2^i \tilde{Q}^j \tilde{t}^c + \lambda_b A_b H_1^i \tilde{Q}^j \tilde{b}^c + \lambda_\tau A_\tau H_1^i \tilde{L}^j \tilde{\tau}^c - \mu B H_1^i H_2^j\right] \tag{2.5}$$

and soft–supersymmetry breaking squark and slepton mass terms

$$M_Q^2[\tilde{t}_L^* \tilde{t}_L + \tilde{b}_L^* \tilde{b}_L] + M_U^2 \tilde{t}_R^* \tilde{t}_R + M_D^2 \tilde{b}_R^* \tilde{b}_R + M_L^2[\tilde{\tau}_L^* \tilde{\tau}_L + \tilde{\nu}_{\tau L}^* \tilde{\nu}_{\tau L}] + M_E^2 \tilde{\tau}_R^* \tilde{\tau}_R \ + \ \cdots \tag{2.6}$$

where the ellipses stand for the soft mass terms corresponding to the first and second generation sfermions.

The minimal SUSY–GUT model emerges by requiring at the GUT scale M_G:

(i) the unification of the U(1), SU(2) and SU(3) coupling constants $\alpha_i = g_i^2/4\pi$ [i = 1–3],

$$\alpha_3(M_\mathrm{G}) = \alpha_2(M_\mathrm{G}) = \alpha_1(M_\mathrm{G}) = \alpha_G \tag{2.7}$$

[1]Note that our convention for the sign of μ is consistent with Ref.[18], which is opposite to the one adopted in Ref.[19].

(ii) a common gaugino mass; the M_i with i =1–3 at the electroweak scale are then related through renormalization group equations (RGEs) to the gauge couplings,

$$M_i = \frac{\alpha_i(M_Z)}{\alpha_G} m_{1/2} \longrightarrow M_3(M_Z) = \frac{\alpha_3(M_Z)}{\alpha_2(M_Z)} M_2(M_Z) = \frac{\alpha_3(M_Z)}{\alpha_1(M_Z)} M_1(M_Z) \tag{2.8}$$

(iii) a universal trilinear coupling A

$$A_G = A_t(M_{\rm G}) = A_b(M_{\rm G}) = A_\tau(M_{\rm G}) \tag{2.9}$$

(iii) a universal scalar mass m_0

$$\begin{aligned} m_0 &= M_Q = M_U = M_D = M_L = M_E \\ &= m_{H_1}(M_G) = m_{H_2}(M_G) \end{aligned} \tag{2.10}$$

Besides the three parameters $m_{1/2}, A_G$ and m_0 the supersymmetric sector is described at the GUT scale by the bilinear coupling B_G and the Higgs–higgsino mass parameter μ_G. The theoretically attractive assumption that the electroweak symmetry is broken radiatively constrains the latter two parameters. Indeed, radiative electroweak symmetry breaking results in two minimization conditions [see Ref.[19] for details] of the Higgs potential; at the low–energy scale in the tree approximation, they are given by

$$\frac{1}{2}M_Z^2 = \frac{m_{H_1}^2 - m_{H_2}^2 \tan^2\beta}{\tan^2\beta - 1} - \mu^2 \tag{2.11}$$

$$B\mu = \frac{1}{2}(m_{H_1}^2 + m_{H_2}^2 + 2\mu^2)\sin 2\beta \tag{2.12}$$

For given values of the GUT parameters $m_{1/2}, m_0, A_G$ as well as $\tan\beta$, the first minimization equation can be solved for μ [to within a sign]; the second equation can then be solved for B. Since $m_{H_1}^2$ and $m_{H_2}^2$ are related to M_A through the RGEs, the solution for μ and B can be approximately expressed as a function of M_A and $\tan\beta$. The power of supergravity models with radiative electroweak symmetry breaking becomes apparent when one includes the one-loop contributions to the Higgs potential. It is through these one–loop terms that most of the supersymmetric particle masses are determined; the minimization conditions [which are also solved for μ to within a sign and B] *fix* the masses in order that the electroweak symmetry is broken correctly, *i.e.* with the correct value of M_Z. [U(1)$_{\rm EM}$ and SU(3) remain unbroken of course]. The one–loop contributions and the minimization equations are given in Ref.[19] to which we refer for details.

A heavy top quark is required to break the electroweak symmetry radiatively, since it is the large top Yukawa coupling which will drive one of the Higgs mass parameters squared to a negative value. As emphasized before, the additional condition of unification of the b–τ Yukawa couplings gives rise to stringent constraints on $\tan\beta$. The attractive idea of explaining the large top Yukawa coupling as a result of a fixed point solution of the RGEs leads to a relationship between M_t and the angle β, $M_t \simeq (200 \text{ GeV})\sin\beta$ for

$\tan\beta \lesssim 10$, giving a further constraint on the model.

To limit the parameter space further, one could require that the SUGRA model is not fine–tuned and the SUSY breaking scale should not be too high, a constraint which can be particularly restrictive in the small $\tan\beta$ region. However, the degree of fine–tuning which can be considered acceptable is largely a matter of taste, so we disregard this issue in our analysis.

We now detail the calculations of the supersymmetric particle spectrum more precisely. We incorporate boundary conditions at both electroweak and GUT scales, adopting the ambidextrous approach of Ref.[19]. We specify the values of the gauge and Yukawa couplings at the electroweak scale, in particular M_t, $\tan\beta$ and α_s. The gauge and Yukawa couplings are then evolved to the GUT scale M_G [defined to be the scale $\tilde{\mu}$ for which $\alpha_1(\tilde{\mu}) = \alpha_2(\tilde{\mu})$] using the two–loop RGEs [13]. At M_G we specify the soft supersymmetry breaking parameters $m_{1/2}$, m_0 and A_G. We then evolve parameters down to the electroweak scale where we apply the one–loop minimization conditions derived from the one–loop effective Higgs potential and solve for μ to within a sign and B [we then can integrate the RGEs back to M_G and obtain μ_G and B_G]. By this procedure, the supersymmetric spectrum is completely specified; that is, we generate a unique spectrum corresponding to particular values of $m_{1/2}$, m_0, A_G, $\tan\beta$ and the sign of μ. It turns out that the spectrum is nearly independent of A_G, for $|A_G| \lesssim 500$ GeV. In most of our calculations, we substitute a particular value of M_A for m_0 in order to introduce a mass parameter which can be measured directly.

We discuss the SUSY spectrum and its phenomenological implications for two representative points in the M_t–$\tan\beta$ plane[2]. We choose $M_t^{\rm pole} = 175$ GeV, consistent with the most recent Tevatron analyses [15] throughout our calculations, and values of $\tan\beta = 1.75$ and 50, which are required (within uncertainties) by b–τ unification at M_G. In particular, we emphasize the low $\tan\beta$ solutions; they are theoretically favored from considerations such as $b \to s\gamma$ [21] and cosmological constraints [22]. The low $\tan\beta$ solutions generate much lighter SUSY spectra, more likely to be seen at future e^+e^- colliders. In both the low and high $\tan\beta$ regions we take[3] $\alpha_s(M_Z) = 0.118$ [23] and $A_G = 0$, though the qualitative behavior in each region should not depend greatly on these parameters.

(a) Low $\tan\beta$

As a typical example of the low $\tan\beta$ region we consider the point $M_t^{\rm pole} = 175$ GeV and $\tan\beta = 1.75$ for which $\lambda_t(M_G)$ lies in its "fixed-point" region [12, 14]. If M_A is fixed, the scalar mass parameter m_0 can be calculated as a function of the common gaugino mass parameter $m_{1/2}$ so that all Higgs and supersymmetric particle masses can in principle be parameterized by $m_{1/2}$. The correlation between m_0 and $m_{1/2}$ is shown in Fig.2 for three

[2] Our numerical analysis is consistent with the numbers obtained in Ref.[20], once their value of A_τ in Tab.X is corrected. We thank W. de Boer for a discussion on this point.

[3] This corresponds to the $\sin^2\theta_W$ value quoted and compared with the high–precision electroweak analyses in the Introduction.

values of $M_A = 300, 600$ and 900 GeV in the low $\tan\beta$ region.

Some of the parameter space is already eliminated by experimental bounds on the light Higgs mass, the chargino/neutralino masses, the light stop mass, the slepton masses and the squark/gluino masses from LEP1/1.5 and the Tevatron [24]. The lower limits are indicated by the non–solid lines in Fig.2. Low values of $m_{1/2} \lesssim 60$ GeV are excluded by the lower bound on the gaugino masses. For $\mu > 0$, the bound from the negative search of charginos at LEP1.5 almost rules out completely the scenario with $M_A \lesssim 300$ GeV. If the h boson is not discovered at LEP2, i.e. if $M_h \gtrsim 95$ GeV, the whole $\mu < 0$ scenario [for $m_{1/2}, m_0 < 500$ GeV] can be excluded, while for $\mu > 0$ only the $m_{1/2} > 200$ GeV range [which implies very large values of M_A] would survive. The requirement that the lightest neutralino is the LSP, and therefore its mass is larger than the lightest $\tilde{\tau}$ mass, excludes a small edge of the parameter space [dotted line] at small m_0 with $m_{1/2} > 200$ GeV in the $\mu < 0$ case.

The masses of the Higgs bosons are shown in Fig.3a as a function of $m_{1/2}$ for $\tan\beta = 1.75$, both signs of μ and for two representative values of $m_0 = 100$ and 500 GeV. The lightest Higgs boson has a rather small tree–level mass and M_h comes mainly from radiative corrections; the maximal values [for $m_{1/2} \sim 400$ GeV] are $M_h^{\rm max} \sim 90$ GeV for $\mu < 0$ and ~ 100 for $\mu > 0$. Because the pseudoscalar mass is approximately given by $M_A^2 \sim B\mu/\sin 2\beta \sim B\mu$ [at the tree–level] and since $B\mu$ turns out to be large in this scenario, the pseudoscalar A is rather heavy especially for large values of m_0, and thus is almost mass degenerate with the heavy CP–even and charged Higgs bosons, $M_A \sim M_H \simeq M_{H^\pm}$. Note that M_A is below the $t\bar{t}$ threshold, $M_A \lesssim 350$ GeV, only if m_0 and $m_{1/2}$ are both of $\mathcal{O}(100)$ GeV.

The chargino/neutralino and sfermion masses are shown Fig.3b-d as a function of $m_{1/2}$ for the two values $M_A = 300$ and 600 GeV and for both signs of μ. In the case of charginos and neutralinos, the masses are related through RGEs by the same ratios that describe the gauge couplings at the electroweak scale. The LSP is almost bino–like [with a mass $m_{\chi_1^0} \sim M_1$] while the next–to–lightest neutralino and the lightest chargino are wino–like [with masses $m_{\chi_2^0} \sim m_{\chi_1^+} \sim M_2 \sim 2m_{\chi_1^0}$]. The heavier neutralinos and chargino are primarily higgsinos with masses $m_{\chi_3^0} \sim m_{\chi_4^0} \sim m_{\chi_2^+} \sim |\mu|$. Note that the masses approximately scale as M_A and that the decay of the heavy scalar and pseudoscalar Higgs bosons into pairs of the heaviest charginos and neutralinos is kinematically not allowed.

The left– and right–handed charged sleptons and sneutrinos are almost mass degenerate, the mass differences not exceeding $\mathcal{O}(10)$ GeV; the mixing in the τ sector is rather small for small $\tan\beta$, allowing one to treat all three generations of sleptons on the same footing. In the case of squarks, only the first two generations are degenerate, with left– and right–handed squarks having approximately the same mass. The mixing in the stop as well as in the sbottom sector leads to a rather substantial splitting between the two stop or sbottom mass eigenstates. Only for small values of M_A and for $\mu < 0$ is $\tilde{b}_1$ the lightest squark; otherwise $\tilde{t}_1$ is the lightest squark state. Note that the squark masses increase with $m_{1/2}$ and that they scale as M_A i.e. as $|\mu|$. The slepton masses decrease with increasing $m_{1/2}$: this is due to the fact that when $m_{1/2}$ increases and M_A is held constant, m_0 decreases [see Fig.2], and the dependence of the slepton masses on m_0 is stronger [for fixed m_0, the slepton masses would increase with increasing $m_{1/2}$].

(b) High $\tan\beta$

In this region we take $\tan\beta = 50$ as a representative example, a value consistent with the unification of the t, b and τ Yukawa couplings. The set of possible solutions in the parameter space $[m_{1/2}, m_0]$ for $M_A = 300$ and 600 GeV is shown in Fig.4. At $\tan\beta = 50$ and $M_t^{\rm pole} = 175$ GeV, we find solutions only for $\mu < 0$; this is a result of the large one–loop contribution to M_A, the sign of which depends on μ [25]. The boundary contours given in the figure correspond to tachyonic solutions in the parameter space: $m^2_{\tilde{\tau}_1} < 0$, $M_A^2 < 0$ or $M_h^2 < 0$ at the tree–level. The latter constraint is important for algorithmic reasons: M_h^2 at the tree–level enters into the minimization equations in the form of a logarithm [19]. Also the requirement of the lightest neutralino to be the LSP excludes a small edge of the parameter space at small values of m_0; this explains why the curves for $M_A = 300$ and 600 GeV do not terminate for low m_0 values.

Particle	Mass (GeV)	Mass (GeV)	Mass (GeV)	Mass (GeV)
M_A	300	300	600	600
$(m_{1/2}, m_0)$	(364,250)	(352,800)	(603,300)	(590,800)
$\tilde{g}$	940	910	1557	1524
$\tilde{t}_1,\tilde{t}_2$	662,817	753,896	1115,1285	1156,1325
$\tilde{b}_1,\tilde{b}_2$	689,787	804,894	1159,1260	1220,1312
$\tilde{u}_1,\tilde{u}_2$	881,909	1144,1164	1431,1479	1586,1628
$\tilde{d}_1,\tilde{d}_2$	878,912	1142,1167	1425,1481	1582,1630
$\tilde{\tau}_1,\ \tilde{\tau}_2;\ \tilde{\nu}_\tau$	165,365; 325	567,740; 729	255,517; 485	586,812; 799
$\tilde{e}_1,\ \tilde{e}_2;\ \tilde{\nu}_e$	290,360; 351	813,838; 835	381,519; 513	833,901; 898
$\chi_i^\pm$	268,498	261,536	452,764	443,779
χ_i^0	144,268,485,496	139,261,526,534	239,452,754,763	234,443,771,778
$M_A,M_{H^\pm},M_H,M_h$	300,315,300,124	300,315,300,124	600,608,600,131	600,608,600,131

Tab.1: Particle spectra for $M_t^{\rm pole} = 175$ GeV, $\tan\beta = 50$ for selected $M_A, m_{1/2}$ and m_0 values.

The sparticle spectra for $M_A = 300$ and 600 GeV and two sets of $m_{1/2}$ and (extreme) m_0 values are shown in Table 1. In all these cases, the particle spectrum is very heavy; hence most of the SUSY decay channels of the Higgs particles are shut for large $\tan\beta$.

The only allowed decay channels are $H, A \to \tilde{\tau}_1\tilde{\tau}_1, \chi_1^0\chi_1^0$ and $H^\pm \to \tilde{\tau}_1\tilde{\nu}$ [for large M_A values]. However, the branching ratios of these decay channels are suppressed by large $b\bar{b}$ and $t\bar{b}$ widths of the Higgs particles for large $\tan\beta$: while the supersymmetric decay widths are of the order $\mathcal{O}(0.1$ GeV), the decays involving b quarks have widths $\mathcal{O}(10$ GeV) and dominate by 2 orders of magnitude.

(c) Additional Constraints

There are additional experimental constraints on the parameter space for both high and low $\tan\beta$; the most important of these are the $b \to s\gamma$, $Z \to b\bar{b}$, and dark matter [relic LSP abundance] constraints. These constraints are much more restrictive in the high $\tan\beta$ case.

Recent studies [21] have indicated that the combination of $b \to s\gamma$, dark matter and m_b constraints disfavor the high $\tan\beta$ solution for which the t, b and τ Yukawa couplings are equal, in particular the minimal SUSY–SO(10) model with universal soft-supersymmetry breaking terms at M_G. This model can, however, be saved if the soft terms are not universal [implying a higgsino–like lightest neutralino], and there exist theoretical motivations for non–universal soft terms at M_G [26]. The presently favored $Z \to b\bar{b}$ decay width would favor a very low A mass for large $\tan\beta$.

For low $\tan\beta$, these additional constraints do not endanger the model, yet they can significantly reduce the available parameter space. In particular the $Z \to b\bar{b}$ constraint favors a light chargino and light stop for small to moderate values of $\tan\beta$ [27, 28] so that they could be detected at LEP2 [28]. The dark matter constraint essentially places an upper limit on m_0 and $m_{1/2}$ [29]. The $b \to s\gamma$ constraint [30], on the other hand, is plagued with large theoretical uncertainties mainly stemming from the unknown next-to-leading QCD corrections and uncertainties in the measurement of $\alpha_s(M_Z)$. However, it is consistent with the low $\tan\beta$ solution and may in the future be useful in determining the sign of μ [31].

3. Production Mechanisms

The main production mechanisms of neutral Higgs bosons at e^+e^- colliders are the Higgs–strahlung process and pair production,

$$\begin{array}{llcl} (a) & \text{Higgs-strahlung} & e^+e^- \to & (Z) \to Z + h/H \\ (b) & \text{pair production} & e^+e^- \to & (Z) \to A + h/H \end{array}$$

as well as the WW and ZZ fusion processes,

$$\begin{array}{llcl} (c) & \text{fusion processes} & e^+e^- \to & \bar{\nu}\nu\,(WW) \to \bar{\nu}\nu\ + h/H \\ & & e^+e^- \to & e^+e^-(ZZ) \to e^+e^- + h/H \end{array}$$

[The $\mathcal{CP}$–odd Higgs boson A cannot be produced in the Higgs–strahlung and fusion processes to leading order since it does not couple to VV pairs.] The charged Higgs particle can be pair produced through virtual photon and Z boson exchange,

$$(d)\ \text{charged Higgs} \qquad e^+e^- \ \to\ (\gamma, Z^*) \ \to\ H^+H^-$$

[For masses smaller than $\sim$ 170 GeV, the charged Higgs boson is also accessible in top decays, $e^+e^- \to t\bar{t}$ with $t \to H^+b$.]

The production cross sections[4] for the neutral Higgs bosons are suppressed by mixing angle factors compared to the SM Higgs production,

$$\sigma(e^+e^- \to Zh)\ ,\ \sigma(VV \to h)\ ,\ \sigma(e^+e^- \to AH) \ \sim\ \sin^2(\beta-\alpha) \tag{3.1}$$
$$\sigma(e^+e^- \to ZH)\ ,\ \sigma(VV \to H)\ ,\ \sigma(e^+e^- \to Ah) \ \sim\ \cos^2(\beta-\alpha) \tag{3.2}$$

while the cross section for the charged Higgs particle does not depend on any parameter other than $M_{H^\pm}$.

In the decoupling limit, $M_A \gg M_Z$, the HVV coupling vanishes, while the hVV coupling approaches the SM Higgs value

$$g_{HVV} \ = \ \cos(\beta-\alpha) \to M_Z^2 \sin 4\beta/2M_A^2 \to 0 \tag{3.3}$$
$$g_{hVV} \ = \ \sin(\beta-\alpha) \to 1 - \mathcal{O}(M_Z^4/M_A^4) \ \ \to 1 \tag{3.4}$$

Hence, the only relevant mechanisms for the production of the heavy Higgs bosons in this limit will be the associated pair production (b) and the pair production of the charged Higgs particles (d). The cross sections, in the decoupling limit and for $\sqrt{s} \gg M_Z$, are given by [we use $M_H \sim M_A$]

$$\sigma(e^+e^- \to AH) \ = \ \frac{G_F^2 M_Z^4}{96\pi s}(v_e^2 + a_e^2)\beta_A^3 \tag{3.5}$$
$$\sigma(e^+e^- \to H^+H^-) \ = \ \frac{2G_F^2 M_W^4 s_W^4}{3\pi s}\left[1 + \frac{v_e v_H}{8 s_W^2 c_W^2} + \frac{(a_e^2 + v_e^2)v_H^2}{256 c_W^4 s_W^4}\right]\beta_{H^\pm}^3 \tag{3.6}$$

where $\beta_j = (1 - 4M_j^2/s)^{1/2}$ is the velocity of Higgs bosons, the Z couplings to electrons are given by $a_e = -1, v_e = -1 + 4\sin^2\theta_W$, and to the charged Higgs boson by $v_H = -2 + 4\sin^2\theta_W$. The cross sections for hA and HZ production vanish in the decoupling limit since they are proportional to $\cos^2(\beta-\alpha)$.

The cross section for the fusion process, $e^+e^- \to \bar{\nu}_e\nu_e H$, is enhanced at high energies since it scales like $M_W^{-2}\log s/M_H^2$. This mechanism provides therefore a useful channel for H production in the mass range of a few hundred GeV below the decoupling limit and small values of $\tan\beta$, where $\cos^2(\beta-\alpha)$ is not prohibitively small; the cross section, though, becomes gradually less important for increasing M_H and vanishes in the decoupling limit.

[4]The complete analytical expressions of the cross sections can be found, e.g., in Ref.[32]. Note that in this paper there are a few typos that we correct here: in eq.(20), the factor 92 should replaced by 96; in the argument of the λ function of the denominator in eq.(21), the parameter M_A^2 should be replaced by M_Z^2; finally, the minus sign in the interference term in eq.(25) should be replaced by a plus sign.

In the high energy regime, the $WW \to H$ fusion cross section is well approximated by the expression

$$\sigma(e^+e^- \to \bar{\nu}_e \nu_e H) = \frac{G_F^3 M_W^4}{4\sqrt{2}\pi^3}\left[\left(1+\frac{M_H^2}{s}\right)\log\frac{s}{M_H^2} - 2\left(1-\frac{M_H^2}{s}\right)\right]\cos^2(\beta-\alpha) \quad (3.7)$$

obtained in the effective longitudinal W approximation. Since the NC couplings are small compared to the CC couplings, the cross section for the ZZ fusion process is $\sim 16\cos^4\theta_W$, *i.e.* one order of magnitude smaller than for WW fusion.

Numerical results for the cross sections are shown in Fig.5 at high–energy e^+e^- colliders as a function of $\sqrt{s}$ TeV for the two values $\tan\beta = 1.75$ and 50, and for pseudoscalar masses $M_A = 300$, 600 and 900 GeV [note that $M_H \simeq M_{H^\pm} \simeq M_A$ as evident from Figs. 1 and 3a]. For a luminosity of $\int\mathcal{L} = 200$ fb^{-1}, typically a sample of about 1000 HA and H^+H^- pairs are predicted for heavy Higgs masses of ~ 500 GeV at $\sqrt{s} = 1.5$ TeV. For small $\tan\beta$ values, $\tan\beta \lesssim 2$, a few hundred events are predicted in the $WW \to H$ fusion process for H masses ~ 300 GeV. The cross sections for the hA and HZ processes are too low, less than ~ 0.1 fb, to be useful for $M_H \gtrsim 300$ GeV; Fig.5b.

Note that the cross sections for the production of the lightest Higgs boson h in the decoupling limit and for $\sqrt{s} \gg M_Z, M_h$ are simply given by

$$\sigma(e^+e^- \to ZZ) \simeq \frac{G_F^2 M_Z^4}{96\pi s}(v_e^2 + a_e^2) \quad (3.8)$$

$$\sigma(e^+e^- \to \bar{\nu}_e \nu_e h) \simeq \frac{G_F^3 M_W^4}{4\sqrt{2}\pi^3}\log\frac{s}{M_h^2} \quad (3.9)$$

The cross sections are the same as for the SM Higgs particle and are very large ~ 100 fb, especially for the WW fusion mechanism.

4. Decay Modes

4.1 Decays to standard particles

For large $\tan\beta$ the Higgs couplings to down–type fermions dominate over all other couplings. As a result, the decay pattern is in general very simple. The neutral Higgs bosons will decay into $b\bar{b}$ and $\tau^+\tau^-$ pairs for which the branching ratios are close to ~ 90 % and ~ 10 %, respectively. The charged Higgs particles decay into $\tau\nu_\tau$ pairs below and into tb pairs above the top–bottom threshold.

The partial decay widths of the neutral Higgs bosons[5], $\Phi = H$ and A, to fermions are given by [4]

$$\Gamma(\Phi \to \bar{f}f) = N_c \frac{G_F M_\Phi}{4\sqrt{2}\pi} g_{\Phi ff}^2 m_f^2 \beta_f^p \quad (4.1)$$

[5]We refrain from a discussion of the h decays which become SM–like in the decoupling limit. In addition, we discuss only the dominant two–body decay modes of the heavy Higgs bosons; for an updated and more detailed discussion, including also three–body decays, see Ref.[33].

with $p=3(1)$ for the CP–even (odd) Higgs bosons; $\beta_f = (1-4m_f^2/M_\Phi^2)^{1/2}$ is the velocity of the fermions in the final state, N_c the color factor. For the decay widths to quark pairs, the QCD radiative corrections are large and must be included; for a recent update and a more detailed discussion, see Ref.[34].

The couplings of the MSSM neutral Higgs bosons [normalized to the SM Higgs coupling $g_{H_{\rm SM}ff} = \left[\sqrt{2}G_F\right]^{1/2} m_f$ and $g_{H_{\rm SM}VV} = 2\left[\sqrt{2}G_F\right]^{1/2} M_V^2$] are given in Table 2.

Φ	$g_{\Phi\bar{u}u}$	$g_{\Phi\bar{d}d}$	$g_{\Phi VV}$
h	$\cos\alpha/\sin\beta$	$-\sin\alpha/\cos\beta$	$\sin(\beta-\alpha)$
H	$\sin\alpha/\sin\beta$	$\cos\alpha/\cos\beta$	$\cos(\beta-\alpha)$
A	$1/\tan\beta$	$\tan\beta$	0

Tab. 2: Higgs boson couplings in the MSSM to fermions and gauge bosons relative to the SM Higgs couplings.

In the decoupling limit, $M_A \gg M_Z$, we have

$$\cos\alpha \sim \sin\beta - \cos\beta \frac{M_Z^2}{2M_A^2}\sin 4\beta \to \sin\beta \tag{4.2}$$

$$\sin\alpha \sim -\cos\beta + \sin\beta \frac{M_Z^2}{2M_A^2}\sin 4\beta \to -\cos\beta \tag{4.3}$$

Therefore the hff couplings reduce to the SM Higgs couplings, while the Hff couplings become equal to those of the pseudoscalar boson A,

$$\begin{aligned} \cos\alpha/\sin\beta &\to 1 \\ -\sin\alpha/\cos\beta &\to 1 \\ -\sin\alpha/\sin\beta &\to 1/\tan\beta \\ \cos\alpha/\cos\beta &\to \tan\beta \end{aligned} \tag{4.4}$$

The partial width of the decay mode $H^+ \to u\bar{d}$ is given by

$$\begin{aligned} \Gamma(H^+ \to u\bar{d}) &= \frac{N_c G_F}{4\sqrt{2}\pi}\frac{\lambda_{ud,H^\pm}^{1/2}}{M_{H^\pm}}|V_{ud}|^2 \times \\ & \left[\left(M_{H^\pm}^2 - m_u^2 - m_d^2\right)\left(m_d^2\tan^2\beta + m_u^2{\rm ctg}^2\beta\right) - 4m_u^2 m_d^2\right] \end{aligned} \tag{4.5}$$

with V_{ud} the CKM–type matrix element for quarks and λ is the two–body phase space function defined by

$$\lambda_{ij,k} = (1 - M_i^2/M_k^2 - M_j^2/M_k^2)^2 - 4M_i^2M_j^2/M_k^4 \tag{4.6}$$

For decays into quark pairs, the QCD corrections must be also included.

Below the $\bar{t}t$ threshold, a variety of channels is open for the decays of the heavy CP–even Higgs bosons, the most important being the cascade decays $H \to \Phi\Phi$ with $\Phi = h$ or A, with a partial width [for real light Higgs bosons]

$$\Gamma(H \to \Phi\Phi) = \frac{G_F}{16\sqrt{2}\pi} \frac{M_Z^4}{M_H} g_{H\Phi\Phi}^2 \beta_\Phi \tag{4.7}$$

where $\beta_\Phi = (1 - 4M_\Phi^2/M_H^2)^{1/2}$ and the radiatively corrected three–boson self–couplings [to leading order], in units of $g'_Z = (\sqrt{2}G_F)^{1/2}M_Z^2$, are given by

$$\begin{aligned} g_{Hhh} &= 2\sin 2\alpha \sin(\beta+\alpha) - \cos 2\alpha \cos(\beta+\alpha) + 3\frac{\epsilon}{M_Z^2}\frac{\sin\alpha\cos^2\alpha}{\sin\beta} \\ g_{HAA} &= -\cos 2\beta \cos(\beta+\alpha) + \frac{\epsilon}{M_Z^2}\frac{\sin\alpha\cos^2\beta}{\sin\beta} \end{aligned} \tag{4.8}$$

In contrast to the previous couplings, the leading m_t^4 radiative corrections cannot be absorbed entirely in the redefinition of the mixing angle α, but they are renormalized by an explicit term depending on the parameter ϵ given by [M_S is the common squark mass at the electroweak scale]

$$\epsilon = \frac{3G_F}{\sqrt{2}\pi^2} \frac{m_t^4}{\sin^2\beta} \log\left(1 + \frac{M_S^2}{m_t^2}\right) \tag{4.9}$$

In the decoupling limit, these couplings approach the values

$$\begin{aligned} g_{Hhh} &\to \frac{3}{2}\sin 4\beta \\ g_{HAA} &\to -\frac{1}{2}\sin 4\beta \end{aligned} \tag{4.10}$$

In the mass range above the WW and ZZ thresholds, where the HVV couplings are not strongly suppressed for small values of $\tan\beta$, the partial widths of the H particle into massive gauge bosons can also be substantial; they are given by

$$\Gamma(H \to VV) = \frac{\sqrt{2}G_F \cos^2(\alpha-\beta)}{32\pi} M_H^3 (1 - 4\kappa_V + 12\kappa_V^2)(1-4\kappa_V)^{1/2}\,\delta'_V \tag{4.11}$$

with $\kappa_V = M_V^2/M_H^2$ and $\delta'_V = 2(1)$ for $V = W(Z)$.

For small values of $\tan\beta$ and below the $\bar{t}t$ and the $t\bar{b}$ thresholds, the pseudoscalar and charged Higgs bosons can decay into the lightest Higgs boson h and a gauge boson; however these decays are suppressed by $\cos^2(\beta-\alpha)$ and therefore are very rare for large A masses. The partial decay widths are given by

$$\begin{aligned} \Gamma(A \to hZ) &= \frac{G_F\cos^2(\beta-\alpha)}{8\sqrt{2}\pi} \frac{M_Z^4}{M_A} \lambda_{Zh,A}^{1/2} \lambda_{Ah,Z} \\ \Gamma(H^+ \to hW^+) &= \frac{G_F\cos^2(\beta-\alpha)}{8\sqrt{2}\pi} \frac{M_W^4}{M_{H^\pm}} \lambda_{Wh,H^\pm}^{\frac{1}{2}} \lambda_{H^\pm h,W} \end{aligned} \tag{4.12}$$

In the decoupling limit, the partial widths of all decays of the heavy CP–even, CP–odd and charged Higgs bosons involving gauge bosons vanish since $\cos^2(\beta-\alpha)\to 0$. In addition, the $H\to hh$ decay width is very small since it is inversely proportional to M_H, and $H\to AA$ is not allowed kinematically. Therefore, the only relevant channels are the decays into $\bar{b}b/\bar{t}t$ for the neutral and $t\bar{b}$ for the charged Higgs bosons. The total decay widths of the three bosons H, A and $H^\pm$, into standard particles can be approximated in this limit by

$$\Gamma(H_k\to \text{all}) = \frac{3G_F}{4\sqrt{2}\pi} M_{H_k}\left[m_b^2 \tan^2\beta + m_t^2 \text{ctg}^2\beta\right] \tag{4.13}$$

[We have neglected the small contribution of the decays into τ leptons for large $\tan\beta$.]

4.2 Decays to charginos and neutralinos

The decay widths of the Higgs bosons H_k [$k=(1,2,3,4)$ correspond to $(H,h,A,H^\pm)$] into neutralino and chargino pairs are given by [35]

$$\Gamma(H_k\to\chi_i\chi_j) = \frac{G_F M_W^2}{2\sqrt{2}\pi}\frac{M_{H_k}\lambda_{ij,k}^{1/2}}{1+\delta_{ij}}\left[(F_{ijk}^2+F_{jik}^2)\left(1-\frac{m_{\chi_i}^2}{M_{H_k}^2}-\frac{m_{\chi_j}^2}{M_{H_k}^2}\right)\right.$$
$$\left. -4\eta_k\epsilon_i\epsilon_j F_{ijk}F_{jik}\frac{m_{\chi_i}m_{\chi_j}}{M_{H_k}^2}\right] \tag{4.14}$$

where $\eta_{1,2,4}=+1$, $\eta_3=-1$ and $\delta_{ij}=0$ unless the final state consists of two identical (Majorana) neutralinos in which case $\delta_{ii}=1$; $\epsilon_i=\pm1$ stands for the sign of the i'th eigenvalue of the neutralino mass matrix [the matrix Z is defined in the convention of Ref.[18], and the eigenvalues of the mass matrix can be either positive or negative] while $\epsilon_i=1$ for charginos; $\lambda_{ij,k}$ is the usual two–body phase space function given in eq.(4.4).

In the case of neutral Higgs boson decays, the coefficients F_{ijk} are related to the elements of the matrices U, V for charginos and Z for neutralinos,

$$H_k\to\chi_i^+\chi_j^- \quad : \quad F_{ijk} = \frac{1}{\sqrt{2}}\left[e_k V_{i1}U_{j2} - d_k V_{i2}U_{j1}\right] \tag{4.15}$$

$$H_k\to\chi_i^0\chi_j^0 \quad : \quad F_{ijk} = \frac{1}{2}\left(Z_{j2}-\tan\theta_W Z_{j1}\right)\left(e_k Z_{i3}+d_k Z_{i4}\right) \; + \; i\leftrightarrow j \tag{4.16}$$

with the coefficients e_k and d_k given by

$$e_1/d_1 = \cos\alpha/-\sin\alpha\ ,\ e_2/d_2=\sin\alpha/\cos\alpha\ ,\ e_3/d_3 = -\sin\beta/\cos\beta \tag{4.17}$$

For the charged Higgs boson, the coupling to neutralino/chargino pairs are given by

$$\begin{aligned} F_{ij4} &= \cos\beta\left[Z_{j4}V_{i1}+\frac{1}{\sqrt{2}}\left(Z_{j2}+\tan\theta_W Z_{j1}\right)V_{i2}\right] \\ F_{ji4} &= \sin\beta\left[Z_{j3}U_{i1}-\frac{1}{\sqrt{2}}\left(Z_{j2}+\tan\theta_W Z_{j1}\right)U_{i2}\right] \end{aligned} \tag{4.18}$$

The matrices U, V for charginos and Z for neutralinos can be found in Ref.[18].

Since in most of the parameter space discussed in Section 2, the Higgs–higgsino mass parameter $|\mu|$ turned out to be very large, $|\mu| \gg M_1, M_2, M_Z$, it is worth discussing the Higgs decay widths into charginos and neutralinos in this limit. First, the decays of the neutral Higgs bosons into pairs of [identical] neutralinos and charginos $H_k \to \chi_i \chi_i$ will be suppressed by powers of M_Z^2/μ^2. This is due to the fact that neutral Higgs bosons mainly couple to *mixtures* of higgsino and gaugino components, and in the large μ limit, neutralinos and charginos are either pure higgsino– or pure gaugino–like. For the same reason, decays $H^+ \to \chi^0_{1,2}\chi_1^+$ and $\chi^0_{3,4}\chi_2^+$ of the charged Higgs bosons will be suppressed. Furthermore, since in this case M_A is of the same order as $|\mu|$, decays into pairs of heavy charginos and neutralinos will be kinematically forbidden. Therefore, the channels

$$\begin{aligned} H, A &\to \chi_1^0 \chi_{3,4}^0\,,\ \chi_2^0\chi_{3,4}^0 \ \text{ and } \chi_1^\pm \chi_2^\mp \\ H^+ &\to \chi_1^+ \chi_{3,4}^0 \ \text{ and } \chi_2^+\chi_{1,2}^0 \end{aligned} \tag{4.19}$$

will be the dominant decay channels of the heavy Higgs particles. Up to the phase space suppression [i.e. for M_A sufficiently larger than $|\mu|$], the partial widths of these decay channels, in units of $G_F M_W^2 M_{H_k}/(4\sqrt{2}\pi)$, are given by [35]

$$\begin{aligned} \Gamma(H \to \chi_1^0\chi_{3,4}^0) &= \frac{1}{2}\tan^2\theta_W(1 \pm \sin 2\beta) \\ \Gamma(H \to \chi_2^0\chi_{3,4}^0) &= \frac{1}{2}(1 \pm \sin 2\beta) \\ \Gamma(H \to \chi_1^\pm \chi_2^\mp) &= 1 \end{aligned} \tag{4.20}$$

$$\begin{aligned} \Gamma(A \to \chi_1^0\chi_{4,3}^0) &= \frac{1}{2}\tan^2\theta_W(1 \pm \sin 2\beta) \\ \Gamma(A \to \chi_2^0\chi_{4,3}^0) &= \frac{1}{2}(1 \pm \sin 2\beta) \\ \Gamma(A \to \chi_1^\pm \chi_2^\mp) &= 1 \end{aligned} \tag{4.21}$$

$$\begin{aligned} \Gamma(H^+ \to \chi_1^+ \chi_{3,4}^0) &= 1 \\ \Gamma(H^+ \to \chi_2^+ \chi_1^0) &= 1 \\ \Gamma(H^+ \to \chi_2^+ \chi_2^0) &= \tan^2\theta_W \end{aligned} \tag{4.22}$$

[We have used the fact that in the decoupling limit $\sin 2\alpha = -\sin 2\beta$.] If all these channels are kinematically allowed, the total decay widths of the heavy Higgs bosons to chargino and neutralino pairs will be given by the expression

$$\Gamma(H_k \to \sum \chi_i\chi_j) = \frac{3G_F M_W^2}{4\sqrt{2}\pi} M_{H_k}\left(1 + \frac{1}{3}\tan^2\theta_W\right) \tag{4.23}$$

which holds universally for all the three Higgs bosons $H, A, H^\pm$.

4.3 Decays to squarks and sleptons

Decays of the neutral and charged Higgs bosons, $H_k = h, H, A, H^\pm$, to sfermion pairs can be written as

$$\Gamma(H_k \to \tilde{f}_i \tilde{f}_j) = \frac{N_C G_F}{2\sqrt{2}\pi M_{H_k}} \lambda^{1/2}_{\tilde{f}_i \tilde{f}_j, H_k} \, g^2_{H_k \tilde{f}_i \tilde{f}_j} \tag{4.24}$$

$\tilde{f}_i$ with $i = 1, 2$ are the sfermion mass eigenstates which are related to the current eigenstates $\tilde{f}_L, \tilde{f}_R$ by

$$\begin{aligned} \tilde{f}_1 &= \tilde{f}_L \cos\theta_f + \tilde{f}_R \sin\theta_f \\ \tilde{f}_2 &= -\tilde{f}_L \sin\theta_f + \tilde{f}_R \cos\theta_f \end{aligned} \tag{4.25}$$

The mixing angles θ_f are proportional to the masses of the partner fermions and they are important only in the case of third generation sfermions. The couplings $g_{H_k \tilde{f}_i \tilde{f}'_j}$ of the neutral and charged Higgs bosons H_k to sfermion mass eigenstates are superpositions of the couplings of the current eigenstates,

$$g_{H_k \tilde{f}_i \tilde{f}'_j} = \sum_{\alpha,\beta = L,R} T_{ij\alpha\beta} \; g_{\Phi \tilde{f}_\alpha \tilde{f}'_\beta} \tag{4.26}$$

The elements of the 4×4 matrix T are given in Tab.3a. The couplings $g_{H_k \tilde{f}_\alpha \tilde{f}'_\beta}$, in the current eigenstate basis $\tilde{f}_{\alpha,\beta} = \tilde{f}_{L,R}$ [normalized to $2(\sqrt{2}G_F)^{1/2}$] may be written as [4, 35]

$$\begin{aligned} g_{H_k \tilde{f}_L \tilde{f}_L} &= m_f^2 g_1^\Phi + M_Z^2 (T_3^f - e_f s_W^2) g_2^\Phi \\ g_{H_k \tilde{f}_R \tilde{f}_R} &= m_f^2 g_1^\Phi + M_Z^2 e_f s_W^2 g_2^\Phi \\ g_{H_k \tilde{f}_L \tilde{f}_R} &= -\frac{1}{2} m_f \left[\mu g_3^\Phi - A_f g_4^\Phi \right] \end{aligned} \tag{4.27}$$

for the neutral Higgs bosons, $H_k = h, H, A$. $T_3 = \pm 1/2$ is the isospin of the [left–handed] sfermion and e_f its electric charge. The coefficients g_i^Φ are given in Tab.3b; in the decoupling limit, the coefficients g_2^Φ reduce to

$$\begin{aligned} \cos(\beta+\alpha) &\to \sin 2\beta \\ \sin(\beta+\alpha) &\to -\cos 2\beta \end{aligned} \tag{4.28}$$

[for the other coefficients, see eqs.(4.2)]. For the charged Higgs bosons, the couplings [also normalized to $2(\sqrt{2}G_F)^{1/2}$] are

$$g_{H^+ \tilde{u}_\alpha \tilde{d}_\beta} = -\frac{1}{\sqrt{2}} \left[g_1^{\alpha\beta} + M_W^2 g_2^{\alpha\beta} \right] \tag{4.29}$$

with the coefficients $g_{1/2}^{\alpha\beta}$ with $\alpha, \beta = L, R$ listed in Table 3c.

i,j / α,β	LL	RR	LR	RL
11	$\cos\theta_f \cos\theta_{f'}$	$\sin\theta_f \sin\theta_{f'}$	$\cos\theta_f \sin\theta_{f'}$	$\sin\theta_f \cos\theta_{f'}$
12	$-\cos\theta_f \sin\theta_{f'}$	$\sin\theta_f \cos\theta_{f'}$	$\cos\theta_f \cos\theta_{f'}$	$-\sin\theta_f \sin\theta_{f'}$
21	$-\sin\theta_f \cos\theta_{f'}$	$\cos\theta_f \sin\theta_{f'}$	$-\sin\theta_f \sin\theta_{f'}$	$\cos\theta_f \cos\theta_{f'}$
22	$\sin\theta_f \sin\theta_{f'}$	$\cos\theta_f \cos\theta_{f'}$	$-\sin\theta_f \cos\theta_{f'}$	$-\cos\theta_f \sin\theta_{f'}$

Tab. 3a: Transformation matrix for the Higgs couplings to sfermions in the presence of mixing.

$\tilde{f}$	Φ	g_1^Φ	g_2^Φ	g_3^Φ	g_4^Φ
	h	$\cos\alpha/\sin\beta$	$-\sin(\alpha+\beta)$	$-\sin\alpha/\sin\beta$	$\cos\alpha/\sin\beta$
$\tilde{u}$	H	$\sin\alpha/\sin\beta$	$\cos(\alpha+\beta)$	$\cos\alpha/\sin\beta$	$\sin\alpha/\sin\beta$
	A	0	0	1	$-1/\tan\beta$
	h	$-\sin\alpha/\cos\beta$	$-\sin(\alpha+\beta)$	$\cos\alpha/\cos\beta$	$-\sin\alpha/\cos\beta$
$\tilde{d}$	H	$\cos\alpha/\cos\beta$	$\cos(\alpha+\beta)$	$\sin\alpha/\cos\beta$	$\cos\alpha/\cos\beta$
	A	0	0	1	$-\tan\beta$

Tab. 3b: Coefficients in the couplings of neutral Higgs bosons to sfermion pairs.

$g_{1/2}^{LL}$	$g_{1/2}^{RR}$	$g_{1/2}^{LR}$	$g_{1/2}^{RL}$
$m_u^2/\tan\beta + m_d^2 \tan\beta$	$m_u m_d(\tan\beta + 1/\tan\beta)$	$m_d(\mu + A_d \tan\beta)$	$m_u(\mu + A_u/\tan\beta)$
$-\sin 2\beta$	0	0	0

Tab. 3c: Coefficients in the couplings of charged Higgs bosons to sfermion pairs.

Mixing between sfermions occurs only in the third–generation sector. For the first two generations the decay pattern is rather simple. In the limit of massless fermions, the pseudoscalar Higgs boson does not decay into sfermions since by virtue of CP–invariance it couples only to pairs of left– and right–handed sfermions with the coupling proportional to m_f. In the asymptotic regime, where the masses $M_{H,H^\pm}$ are large, the decay widths of the heavy CP–even and charged [36] Higgs bosons into sfermions are proportional to

$$\Gamma(H, H^+ \to \tilde{f}\tilde{f}) \sim \frac{G_F M_W^4}{M_H} \sin^2 2\beta \tag{4.30}$$

These decay modes can be significant only for low values $\tan\beta$ [which implies $\sin^2 2\beta \sim 1$]. However, in this regime the decay widths are inversely proportional to M_H, and thus cannot compete with the decay widths into charginos/neutralinos and ordinary fermions which increase with increasing Higgs mass. Therefore, the decays into first and second generations are unlikely to be important.

In the case of the third generation squarks, the Higgs decay widths can be larger by more than an order of magnitude. For instance the decay widths of the heavy neutral Higgs boson into top squarks of the same helicity is proportional to

$$\Gamma(H \to \tilde{t}\tilde{t}) \sim \frac{G_F m_t^4}{M_H \tan^2\beta} \tag{4.31}$$

in the asymptotic region, and it will be enhanced by large coefficients [for small $\tan\beta$] compared to first/second generation squarks. Conversely, the decay widths into sbottom quarks can be very large for large $\tan\beta$. Furthermore, the decays of heavy neutral CP–even and CP–odd Higgs bosons to top squarks of different helicities will be proportional in the asymptotic region [and for the CP–even, up to the suppression by mixing angle] to

$$\Gamma(H, A \to \tilde{t}\tilde{t}) \sim \frac{G_F m_t^2}{M_H} \left[\mu + A_t/\tan\beta\right]^2 \tag{4.32}$$

For μ and A_t values of the order of the Higgs boson masses, these decay widths will be competitive with the chargino/neutralino and standard fermion decays. Therefore, if kinematically allowed, these decay modes have to be taken into account.

4.4 Numerical results

The decay widths of the H, A and $H^\pm$ Higgs bosons into the sum of charginos and neutralinos, squark or slepton final states, as well as the standard and the total decay widths are shown in Figs.6a, 7a and 8a as a function of $m_{1/2}$ for two values of the pseudoscalar Higgs boson mass $M_A = 300$ and 600 GeV, and for positive and negative μ values; $\tan\beta$ is fixed to 1.75.

Fig.6a shows the various decay widths for the heavy CP–even Higgs boson. For $M_A = 300$ GeV, the $H \to t\bar{t}$ channel is still closed and the decay width into standard particles is rather small, being of $\mathcal{O}(250)$ MeV. In this case, the decays into the lightest stop squarks which are kinematically allowed for small values of $m_{1/2}$ will be by far the dominant decay channels. This occurs in most of the $m_{1/2}$ range if $\mu > 0$, but if $\mu < 0$ only for $m_{1/2} \lesssim 50$ GeV which is already ruled out by CDF and LEP1.5 data.

The decays into charginos and neutralinos, although one order of magnitude smaller than stop decays when allowed kinematically, are also very important. They exceed the standard decays in most of the $m_{1/2}$ range, except for large values of $m_{1/2}$ and $\mu < 0$ where no more phase space is available for the Higgs boson to decay into combinations of the heavy and light chargino/neutralino states. For small $m_{1/2}$ values, chargino and neutralino decays can be larger than the standard decays by up to an order of magnitude.

As expected, the decay widths into sleptons are rather small and they never exceed the widths into standard particles, except for large values of $m_{1/2}$. Note that due to the isospin and charge assignments, the coupling of the H boson to sneutrinos is approximately a factor of two larger than the coupling to the charged sleptons. Since all the sleptons of the three generations are approximately mass degenerate [the mixing in the $\tilde{\tau}$ sector is very small for low values of $\tan\beta$], the small decay widths into sleptons are given by the approximate relation: $\Gamma(H \to \tilde{\nu}\tilde{\nu}) \simeq 4\Gamma(H \to \tilde{l}_L\tilde{l}_L) \simeq 4\Gamma(H \to \tilde{l}_R\tilde{l}_R)$.

For larger values of M_H, $M_H \gtrsim 350$ GeV, the decay widths into supersymmetric particles have practically the same size as discussed previously. However, since the $H \to t\bar{t}$ channel opens up, the decay width into standard model particles becomes rather large, $\mathcal{O}(10$ GeV$)$, and the supersymmetric decays are no longer dominant. For $M_H \simeq 600$ GeV, Fig.6a, only the $H \to \tilde{q}\tilde{q}$ decay width can be larger than the decay width to standard particles; this occurs in the lower range of the $m_{1/2}$ values. The chargino/neutralino decays have a branching ratio of $\sim 20\%$, while the branching ratios of the decays into sleptons are below the 1% level.

Fig.6b and 6c show the individual decay widths of the heavy H boson with a mass $M_H \simeq 600$ GeV into charginos, neutralinos, stop quarks and sleptons for the set of parameters introduced previously. For decays into squarks, only the channels $H \to \tilde{t}_1\tilde{t}_1, \tilde{t}_1\tilde{t}_2$, and in a very small range of $m_{1/2}$ values the channel $H \to \tilde{b}_1\tilde{b}_1$, are allowed kinematically [see Fig.3c]. The decay into two different stop states is suppressed by the [small] mixing angle, and due to the larger phase space the decay $H \to \tilde{t}_1\tilde{t}_1$ is always dominating.

For the decays into chargino and neutralinos, the dominant channels are decays into mixtures of light and heavy neutralinos and charginos, in particular $H \to \chi_1^+\chi_2^-$ and $H \to \chi_1^0\chi_3^0$ or $\chi_2^0\chi_3^0$. This can be qualitatively explained, up to phase space suppression factors, by recalling the approximate values of the relative branching ratios in the large $|\mu|$ limit given in eqs.(4.18–20): $\Gamma(H \to \chi_1^\pm\chi_2^\mp) \sim 1$, while $\Gamma(H \to \chi_2^0\chi_3^0) \sim 1$ and $\Gamma(H \to \chi_1^0\chi_3^0) \sim \tan^2\theta_W$ because $\sin 2\beta$ is close to one. The mixed decays involving χ_4^0 are suppressed since they are proportional to $(1 - \sin 2\beta)$, and all other decay channels are suppressed by powers of M_Z^2/μ^2 for large $|\mu|$ values.

The decay widths for the pseudoscalar Higgs boson are shown in Fig.7a. There are no decays into sleptons, since the only decay allowed by CP–invariance, $A \to \tilde{\tau}_1\tilde{\tau}_2$, is strongly suppressed by the very small $\tilde{\tau}$ mixing angle. For $M_A = 300$ GeV, the decay into the two stop squark eigenstates, $A \to \tilde{t}_1\bar{\tilde{t}}_2$, is not allowed kinematically and the only possible supersymmetric decays are the decays into charginos and neutralinos. The sum of the decay widths into these states can be two orders of magnitude larger than the decay width into standard particles.

For values of M_A above the $t\bar{t}$ threshold, the decay width into charginos and neutralinos is still of the same order as for low M_A, but because of the opening of the $A \to t\bar{t}$ mode, the total decay width increases dramatically and the chargino/neutralino decay branching ratio drops to the level of 20%. As in the case of the heavy CP–even Higgs boson H, the relative decay widths of the pseudoscalar boson into charginos and neutralinos, Fig.7b, are larger for the channels involving mixtures of light and heavy neutralinos or charginos; the dominant decay modes are, roughly, $A \to \chi_1^+\chi_2^-$ and $A \to \chi_1^0\chi_4^0$ or $\chi_2^0\chi_4^0$. Again, this can be qualitatively explained, up to phase space suppression factors, by recalling the approximate formulae of eqs.(4.18–19), since the situation is the same as for H, with the two neutralino states χ_3^0 and χ_4^0 being interchanged.

For small values of the common gaugino mass, $m_{1/2} \lesssim 100$ GeV, the decay mode of the pseudoscalar Higgs boson into stop squarks, $A \to \tilde{t}_1\bar{\tilde{t}}_2$, is phase space allowed. In this case, it is competitive with the top–antitop decay mode. As discussed previously, the $1/M_A^2$ suppression [and to a lesser extent the suppression due to the mixing angle] of the $A \to \tilde{t}_1\bar{\tilde{t}}_2$ decay width compared to $\Gamma(A \to t\bar{t})$ will be compensated by the enhancement of the $A\tilde{t}_1\bar{\tilde{t}}_2$ coupling for large values of μ and A_t.

Fig.8a shows the decay widths for the charged Higgs boson. Since the dominant decay channel $H^+ \to t\bar{b}$ is already open for $M_{H^\pm} \simeq 300$ GeV [although still slightly suppressed by phase space], the charged Higgs decay width into standard particles is rather large and it increases only by a factor of ~ 4 when increasing the pseudoscalar mass to $M_A = 600$ GeV. The situation for the supersymmetric decays is quite similar for the two masses: the chargino/neutralinos decay modes have branching ratios of the order of a few ten percent, while the branching ratios for the decays into sleptons, when kinematically allowed, do not exceed the level of a few percent, as expected. Only the decay $H^+ \to \tilde{t}_1\bar{\tilde{b}}_1$, the only squark decay mode allowed by phase space [see Fig.3c] for relatively low values of $m_{1/2}$, is competitive with the $t\bar{b}$ decay mode.

The decay widths of the charged Higgs into the various combinations of charginos and neutralinos are shown in Fig.8b for $M_{H^\pm} \sim 600$ GeV. The dominant channels are again decays into mixtures of gauginos and higgsinos, since $|\mu|$ is large. The pattern follows approximately the rules of eq.(4.22), modulo phase suppression.

As discussed in section 2, since the chargino, neutralino and sfermion masses scale as M_A, the situation for even larger values of the pseudoscalar Higgs boson mass, $M_A \sim 1$ TeV, will be qualitatively similar to what has been discussed for $M_A \sim 600$ GeV. The only exception is that there will be slightly more phase space available for the supersymmetric decays to occur.

5. Final Decay Products of the Higgs Bosons

In this section, we will qualitatively describe the final decay products of the produced Higgs bosons. Assuming that M_A is large, $M_A \gtrsim 500$ GeV, the decays into standard particles [and more precisely, the $t\bar{t}$ for the neutral and the $t\bar{b}$ decays for the charged Higgs bosons] always have substantial branching ratios, even for the value $\tan\beta = 1.75$ which will be chosen for the discussion. Therefore, to investigate decays into SUSY particles in the main production processes, $e^+e^- \to HA$ and H^+H^-, one has to look for final states where one of the Higgs bosons decays into standard modes while the other Higgs boson decays into charginos, neutralinos or stop squarks. As discussed previously, the decays into the other squarks are disfavored by phase space, while the branching ratios into sleptons are always small and can be neglected.

Let us first discuss the case where one of the Higgs bosons decays into chargino and neutralino pairs,

$$\begin{aligned} e^+e^- &\to H\ A \to [t\bar{t}]\,[\chi^+\chi^-] \ \text{ and } \ [t\bar{t}]\,[\chi^0\chi^0] \\ e^+e^- &\to H^+H^- \to [tb]\,[\chi^\pm\chi^0] \end{aligned} \tag{5.1}$$

The lightest chargino χ_1^+ and next–to–lightest neutralino χ_2^0 decay into [possibly virtual] W, Z and the lightest Higgs boson h, assuming that decays into sleptons and squarks are kinematically disfavored. In the limit of large $|\mu|$, the decay widths [in the decoupling limit] are proportional to [37]

$$\Gamma(\chi_1^+ \to \chi_1^0 W^+) \sim \sin^2 2\beta \tag{5.2}$$

$$\begin{aligned} \Gamma(\chi_2^0 \to \chi_1^0 Z) &\sim \cos^2 2\beta\,[(M_2-M_1)/2\mu]^2 \\ \Gamma(\chi_2^0 \to \chi_1^0 h) &\sim \sin^2 2\beta \end{aligned} \tag{5.3}$$

In most of the parameter space, the $W/Z/h$ are virtual [in addition to the three–body phase space factors, the decay widths are suppressed by powers of $M_2 M_Z/\mu^2$] except near the upper values of $m_{1/2}$. In the case of χ_2^0, the channel $\chi_2^0 \to \chi_1^0 Z$ mode is always dominant although suppressed by additional powers of M_2^2/μ^2 compared to the $\chi_2^0 \to h\chi_1^0$ mode, since both h and Z are off–shell, and the Z boson width is much larger than the width of the h boson for small values of $\tan\beta$. The radiative decay $\chi_2^0 \to \chi_1^0\gamma$ should play a marginal role except for very small values of $m_{1/2}$ where the difference between the χ_2^0 and Z boson masses becomes too large.

For large values of $m_{1/2}$, the sleptons become rather light compared to the gauginos and the decays of the light chargino and neutralino into leptons+sleptons are kinematically possible. In this case, these cascade decays become dominant since the partial widths for large $|\mu|$ are given by

$$\sum_l \Gamma(\chi_2^0 \to l\tilde{l}) = \sum_l 2\Gamma(\chi_1^\pm \to l\tilde{\nu}) = \frac{3G_F^2 M_W^2}{\sqrt{2}\pi} M_2 \tag{5.4}$$

and therefore not suppressed by powers of $M_Z M_2/\mu^2$, unlike the previous decay modes [we assume of course that there is no suppression by phase–space]. The sleptons will then decay into the LSP and massless leptons, leading to multi–lepton final states.

The heavier chargino, in the absence of squark and slepton decay modes, will decay preferentially into the lightest chargino and neutralinos plus gauge or light Higgs bosons. The decay widths, in units of $G_F M_W^2|\mu|/(8\sqrt{2}\pi)$ may be approximated in the decoupling limit by [37]

$$\chi_2^+ \ \to \ \chi_1^+ Z \ : \ \Gamma = 1$$

$$
\begin{aligned}
&\rightarrow \quad \chi_1^+ h \quad : \Gamma = 1 \\
&\rightarrow \quad \chi_1^0 W^+ \quad : \Gamma = \tan^2\theta_W \\
&\rightarrow \quad \chi_2^0 W^+ \quad : \Gamma = 1
\end{aligned} \tag{5.5}
$$

The branching ratios for the various final states are roughly equal. Since χ_2^+ is almost higgsino–like, the decay widths into sleptons and partners of the light quarks, when kinematically allowed, are extremely small since they are suppressed by powers of m_f^2/M_Z^2. Because of the large m_t value, only the decays into stop squarks and bottom quarks will be very important. This decay is allowed in most of the parameter space for $M_A \gtrsim 600$ GeV and, up to suppression by mixing angles, it is enhanced by a power m_t^2 [37]

$$
\frac{\Gamma(\chi_2^+ \rightarrow \tilde{t}b)}{\Gamma(\chi_2^+ \rightarrow W, Z, h)} \sim \frac{3m_t^2}{M_W^2} \frac{1}{\sin^2\beta(3+\tan^2\theta_W)} \sim 4 \tag{5.6}
$$

compared to the other decays. Therefore, when kinematically possible, this decay will be the dominant decay mode of the heavy charginos.

For the heavier neutralinos, $\chi_{3,4}^0$, the decay widths into $W/Z/h$ bosons, again in units of $G_F M_W^2 |\mu|/(8\sqrt{2}\pi)$ may be be written in the decoupling limit as [37]

$$
\begin{aligned}
\chi_{3/4}^0 \quad &\rightarrow \quad \chi_1^0 Z \quad : \Gamma = \frac{1}{2}\tan^2\theta_W(1 \pm \sin 2\beta) \\
&\rightarrow \quad \chi_1^0 h \quad : \Gamma = \frac{1}{2}\tan^2\theta_W(1 \mp \sin 2\beta) \\
&\rightarrow \quad \chi_2^0 Z \quad : \Gamma = \frac{1}{2}(1 \pm \sin 2\beta) \\
&\rightarrow \quad \chi_2^0 h \quad : \Gamma = \frac{1}{2}(1 \mp \sin 2\beta) \\
&\rightarrow \quad \chi_1^+ W^- \quad : \Gamma = 2
\end{aligned} \tag{5.7}
$$

The dominant mode is the charged decay, $\chi_{3,4}^0 \rightarrow \chi_1^+ W^-$, followed by the modes involving the $h(Z)$ boson for $\chi_4^0(\chi_3^0)$. Because $\sin 2\beta \sim 1$, only one of the h or Z decay channels is important. Here again, because of the higgsino nature of the two heavy neutralinos, the decay widths into sleptons and the scalar partners of the light quarks are negligible; the only important decays are the stop decays, $\chi_{3,4}^0 \rightarrow t\tilde{t}_1$, when they are allowed kinematically [i.e. for not too large values of $m_{1/2}$]. The ratio between stop and $W/Z/h$ decay widths, up to suppression by mixing angles, is also given by eq.(5.6), and the stop decays will therefore dominate.

We now turn to the case where one of the produced Higgs particles decays into stop squarks

$$
\begin{aligned}
e^+e^- \quad &\rightarrow \quad H\ A \rightarrow [t\bar{t}]\,[\tilde{t}_1\tilde{t}_1] \ \text{ and } \ [t\bar{t}]\,[\tilde{t}_1\tilde{t}_2] \\
e^+e^- \quad &\rightarrow \quad H^+H^- \rightarrow [tb][\tilde{t}_1\tilde{b}_1]
\end{aligned} \tag{5.8}
$$

From the squark mass plots, Fig. 3c, the only decay modes of the lightest stop squark allowed by phase space are

$$\tilde{t}_1 \to t\chi_1^0 \quad , \quad t\chi_2^0 \quad , \quad b\chi_1^+ \tag{5.9}$$

Only the last decay mode occurs for relatively small values of $m_{1/2}$, since $m_{\tilde{t}_1} < m_t + m_{\chi^0_{1,2}}$ in this case. For larger values of $m_{1/2}$, $\tilde{t}_1$ is heavy enough to decay into top quarks plus the lightest neutralinos. For these $m_{1/2}$ values, the three decay modes of eq.(5.9) will have approximately the same magnitude since the chargino and the neutralinos are gaugino–like and there is no enhancement due to the top mass for the $\tilde{t}_1 \to t\chi^0$ decays.

The heavier stop squark, in addition to the previous modes, has decay channels with $\tilde{t}_1$ and Z/h bosons in the final state

$$\tilde{t}_2 \to \tilde{t}_1 Z \quad , \quad \tilde{t}_1 h \tag{5.10}$$

These decays, in particular the decay into the lightest Higgs boson h, will be dominant in the large $|\mu|$ limit, since they will be enhanced by powers of μ^2.

Appendix A: Chargino and Neutralino Masses and Couplings

In this Appendix we collect the analytical expressions of the chargino and neutralino masses and couplings, and we discuss the limit in which the Higgs–higgsino mass parameter $|\mu|$ is large.

The general chargino mass matrix [18],

$$\mathcal{M}_C = \begin{bmatrix} M_2 & \sqrt{2} M_W \sin\beta \\ \sqrt{2} M_W \cos\beta & \mu \end{bmatrix} \tag{A1}$$

is diagonalized by two real matrices U and V,

$$U^* \mathcal{M}_C V^{-1} \quad \to \quad U = \mathcal{O}_- \text{ and } V = \begin{cases} \mathcal{O}_+ & \text{if } \det\mathcal{M}_C > 0 \\ \sigma\mathcal{O}_+ & \text{if } \det\mathcal{M}_C < 0 \end{cases} \tag{A2}$$

where σ is the matrix

$$\sigma = \begin{bmatrix} \pm 1 & 0 \\ 0 & \pm 1 \end{bmatrix} \tag{A3}$$

with the appropriate signs depending upon the values of M_2, μ, and $\tan\beta$ in the chargino mass matrix. $\mathcal{O}_\pm$ is given by:

$$\mathcal{O}_\pm = \begin{bmatrix} \cos\theta_\pm & \sin\theta_\pm \\ -\sin\theta_\pm & \cos\theta_\pm \end{bmatrix} \tag{A4}$$

with

$$\begin{aligned}\tan 2\theta_- &= \frac{2\sqrt{2}M_W(M_2\cos\beta+\mu\sin\beta)}{M_2^2-\mu^2-2M_W^2\cos\beta}\\ \tan 2\theta_+ &= \frac{2\sqrt{2}M_W(M_2\sin\beta+\mu\cos\beta)}{M_2^2-\mu^2+2M_W^2\cos\beta}\end{aligned}\tag{A5}$$

This leads to the two chargino masses, the $\chi_{1,2}^+$ masses

$$\begin{aligned}m_{\chi_{1,2}^+} = &\frac{1}{\sqrt{2}}\Big[M_2^2+\mu^2+2M_W^2\\ &\mp\Big\{(M_2^2-\mu^2)^2+4M_W^4\cos^2 2\beta+4M_W^2(M_2^2+\mu^2+2M_2\mu\sin 2\beta)\Big\}^{\frac{1}{2}}\Big]^{\frac{1}{2}}\end{aligned}\tag{A6}$$

In the limit $|\mu|\gg M_2, M_Z$, the masses of the two charginos reduce to

$$\begin{aligned}m_{\chi_1^+} &\simeq M_2-\frac{M_W^2}{\mu^2}\left(M_2+\mu\sin 2\beta\right)\\ m_{\chi_2^+} &\simeq |\mu|+\frac{M_W^2}{\mu^2}\epsilon_\mu\left(M_2\sin 2\beta+\mu\right)\end{aligned}\tag{A7}$$

where ϵ_μ is for the sign of μ. For $|\mu|\to\infty$, the lightest chargino corresponds to a pure wino state with mass $m_{\chi_1^+}\simeq M_2$, while the heavier chargino corresponds to a pure higgsino state with a mass $m_{\chi_1^+}=|\mu|$.

In the case of the neutralinos, the four-dimensional neutralino mass matrix depends on the same two mass parameters μ and M_2, if the GUT relation $M_1=\frac{5}{3}\tan^2\theta_W\ M_2\simeq\frac{1}{2}M_2$ [18] is used. In the $(-i\tilde{B}, -i\tilde{W}_3, \tilde{H}_1^0, \tilde{H}_2^0)$ basis, it has the form

$$\mathcal{M}_N=\begin{bmatrix} M_1 & 0 & -M_Z s_W\cos\beta & M_Z s_W\sin\beta\\ 0 & M_2 & M_Z c_W\cos\beta & -M_Z c_W\sin\beta\\ -M_Z s_W\cos\beta & M_Z c_W\cos\beta & 0 & -\mu\\ M_Z s_W\sin\beta & -M_Z c_W\sin\beta & -\mu & 0\end{bmatrix}\tag{A8}$$

It can be diagonalized analytically [38] by a single real matrix Z; the [positive] masses of the neutralino states $m_{\chi_i^0}$ are given by

$$\begin{aligned}\epsilon_1 m_{\chi_1^0} &= C_1-\left(\frac{1}{2}a-\frac{1}{6}C_2\right)^{1/2}+\left[-\frac{1}{2}a-\frac{1}{3}C_2+\frac{C_3}{(8a-8C_2/3)^{1/2}}\right]^{1/2}\\ \epsilon_2 m_{\chi_2^0} &= C_1+\left(\frac{1}{2}a-\frac{1}{6}C_2\right)^{1/2}-\left[-\frac{1}{2}a-\frac{1}{3}C_2-\frac{C_3}{(8a-8C_2/3)^{1/2}}\right]^{1/2}\\ \epsilon_3 m_{\chi_3^0} &= C_1-\left(\frac{1}{2}a-\frac{1}{6}C_2\right)^{1/2}-\left[-\frac{1}{2}a-\frac{1}{3}C_2+\frac{C_3}{(8a-8C_2/3)^{1/2}}\right]^{1/2}\\ \epsilon_4 m_{\chi_4^0} &= C_1+\left(\frac{1}{2}a-\frac{1}{6}C_2\right)^{1/2}+\left[-\frac{1}{2}a-\frac{1}{3}C_2-\frac{C_3}{(8a-8C_2/3)^{1/2}}\right]^{1/2}\end{aligned}\tag{A9}$$

where $\epsilon_i = \pm 1$; the coefficients C_i and a are given by

$$\begin{aligned}
C_1 &= (M_1 + M_2)/4 \\
C_2 &= M_1 M_2 - M_Z^2 - \mu^2 - 6C_1^2 \\
C_3 &= 2C_1 \left[C_2 + 2C_1^2 + 2\mu^2 \right] + M_Z^2 (M_1 c_W^2 + M_2 s_W^2) - \mu M_Z^2 \sin 2\beta \\
C_4 &= C_1 C_3 - C_1^2 C_2 - C_1^4 - M_1 M_2 \mu^2 + (M_1 c_W^2 + M_2 s_W^2) M_Z^2 \mu \sin 2\beta
\end{aligned} \quad \text{(A10)}$$

and

$$a = \frac{1}{2^{1/3}} \mathrm{Re} \left[S + i \left(\frac{D}{27} \right)^{1/2} \right]^{1/3} \quad \text{(A11)}$$

with

$$\begin{aligned}
S &= C_3^2 + \frac{2}{27} C_2^3 - \frac{8}{3} C_2 C_4 \\
D &= \frac{4}{27} (C_2^2 + 12 C_4)^3 - 27 S^2
\end{aligned} \quad \text{(A12)}$$

In the limit of large $|\mu|$ values, the masses of the neutralino states simplify to

$$\begin{aligned}
m_{\chi_1^0} &\simeq M_1 - \frac{M_Z^2}{\mu^2} (M_1 + \mu \sin 2\beta)\, s_W^2 \\
m_{\chi_2^0} &\simeq M_2 - \frac{M_Z^2}{\mu^2} (M_2 + \mu \sin 2\beta)\, c_W^2 \\
m_{\chi_3^0} &\simeq |\mu| + \frac{1}{2} \frac{M_Z^2}{\mu^2} \epsilon_\mu (1 - \sin 2\beta) \left(\mu + M_2 s_W^2 + M_1 c_W^2 \right) \\
m_{\chi_4^0} &\simeq |\mu| + \frac{1}{2} \frac{M_Z^2}{\mu^2} \epsilon_\mu (1 + \sin 2\beta) \left(\mu - M_2 s_W^2 - M_1 c_W^2 \right)
\end{aligned} \quad \text{(A13)}$$

Again, for $|\mu| \to \infty$, two neutralinos are pure gaugino states with masses $m_{\chi_1^0} \simeq M_1$, $m_{\chi_2^0} = M_2$, while the two others are pure higgsino states, with masses $m_{\chi_3^0} \simeq m_{\chi_4^0} \simeq |\mu|$.

The matrix elements of the diagonalizing matrix, Z_{ij} with $i,j = 1,..4$, are given by

$$\begin{aligned}
Z_{i1} &= \left[1 + \left(\frac{Z_{i2}}{Z_{i1}} \right)^2 + \left(\frac{Z_{i3}}{Z_{i1}} \right)^2 + \left(\frac{Z_{i4}}{Z_{i1}} \right)^2 \right]^{-1/2} \quad \text{(A14)} \\
\frac{Z_{i2}}{Z_{i1}} &= -\frac{1}{\tan \theta_W} \frac{M_1 - \epsilon_i m_{\chi_i^0}}{M_2 - \epsilon_i m_{\chi_i^0}} \\
\frac{Z_{i3}}{Z_{i1}} &= \frac{\mu (M_1 - \epsilon_i m_{\chi_i^0})(M_2 - \epsilon_i m_{\chi_i^0}) - M_Z^2 \sin\beta \cos\beta [(M_1 - M_2) c_W^2 + M_2 - \epsilon_i m_{\chi_i^0}]}{M_Z (M_2 - \epsilon_i m_{\chi_i^0}) s_W [\mu \cos\beta + \epsilon_i m_{\chi_i^0} \sin\beta)} \\
\frac{Z_{i4}}{Z_{i1}} &= \frac{-\epsilon_i m_{\chi_i^0} (M_1 - \epsilon_i m_{\chi_i^0})(M_2 - \epsilon_i m_{\chi_i^0}) - M_Z^2 \cos^2\beta [(M_1 - M_2) c_W^2 + M_2 - \epsilon_i m_{\chi_i^0}]}{M_Z (M_2 - \epsilon_i m_{\chi_i^0}) s_W [\mu \cos\beta + \epsilon_i m_{\chi_i^0} \sin\beta)}
\end{aligned}$$

where ϵ_i is the sign of the ith eigenvalue of the neutralino mass matrix, which in the large $|\mu|$ limit are: $\epsilon_1 = \epsilon_2 = 1$ and $\epsilon_4 = -\epsilon_3 = \epsilon_\mu$.

Appendix B: Sfermion Masses and Mixing

We now present the explicit expressions of the squark and slepton masses. We will assume a universal scalar mass m_0 and gaugino mass $m_{1/2}$ at the GUT scale, and we will neglect the Yukawa couplings in the RGE's [see Appendix C]. For third generation squarks this is a poor approximation since these couplings can be large; these have been taken into account in the numerical analysis.

By performing the RGE evolution to the electroweak scale, one obtains for the left– and right–handed sfermion masses at one–loop order [we include the full two–loop evolution of the masses in the numerical analysis]

$$m^2_{\tilde{f}_{L,R}} = m_0^2 + \sum_{i=1}^{3} F_i(f) m^2_{1/2} \pm (T_{3f} - e_f s_W^2) M_Z^2 \cos 2\beta \tag{B1}$$

T_{3f} and e_f are the weak isospin and the electric charge of the corresponding fermion f, and F_i are the RGE coefficients for the three gauge couplings at the scale $Q \sim M_Z$, given by

$$F_i = \frac{c_i(f)}{b_i} \left[1 - \left(1 - \frac{\alpha_G}{4\pi} b_i \log \frac{Q^2}{M_G^2} \right)^{-2} \right] \tag{B2}$$

The coefficients b_i, assuming that all the MSSM particle spectrum contributes to the evolution from Q to the GUT scale M_G, are

$$b_1 = 33/5 \quad , \quad b_2 = 1 \quad , \quad b_3 = -3 \tag{B3}$$

The coefficients $c(\tilde{f}) = (c_1, c_2, c_3)(\tilde{f})$ depend on the hypercharge and color of the sfermions [$F_L = L_L$ or Q_L is the slepton or squark doublet]

$$c(\tilde{L}_L) = \begin{pmatrix} 3/10 \\ 3/2 \\ 0 \end{pmatrix} \quad , \quad c(\tilde{E}_R) = \begin{pmatrix} 6/5 \\ 0 \\ 0 \end{pmatrix}$$

$$c(\tilde{Q}_L) = \begin{pmatrix} 1/30 \\ 3/2 \\ 8/3 \end{pmatrix} \quad , \quad c(\tilde{U}_R) = \begin{pmatrix} 8/15 \\ 0 \\ 8/3 \end{pmatrix} \quad , \quad c(\tilde{D}_R) = \begin{pmatrix} 2/15 \\ 0 \\ 8/3 \end{pmatrix} \tag{B4}$$

With the input gauge coupling constants at the scale of the Z boson mass

$$\alpha_1(M_Z) \simeq 0.01 \quad , \quad \alpha_2(M_Z) \simeq 0.033 \quad , \quad \alpha_3(M_Z) \simeq 0.118 \tag{B5}$$

one obtains for the GUT scale M_G and for the coupling constant α_G

$$M_G \sim 1.9 \times 10^{16} \text{ GeV} \quad \text{and} \quad \alpha_G = 0.041 \tag{B6}$$

Using these values, and including only gauge loops in the one–loop RGE's, one obtains for the left– and right–handed sfermion masses [39]

$$\begin{aligned}
m^2_{\tilde{u}_L} &= m_0^2 + 6.28 m^2_{1/2} + 0.35 M_Z^2 \cos(2\beta) \\
m^2_{\tilde{d}_L} &= m_0^2 + 6.28 m^2_{1/2} - 0.42 M_Z^2 \cos(2\beta) \\
m^2_{\tilde{u}_R} &= m_0^2 + 5.87 m^2_{1/2} + 0.16 M_Z^2 \cos(2\beta) \\
m^2_{\tilde{d}_R} &= m_0^2 + 5.82 m^2_{1/2} - 0.08 M_Z^2 \cos(2\beta) \\
m^2_{\tilde{\nu}_L} &= m_0^2 + 0.52 m^2_{1/2} + 0.50 M_Z^2 \cos(2\beta) \\
m^2_{\tilde{e}_L} &= m_0^2 + 0.52 m^2_{1/2} - 0.27 M_Z^2 \cos(2\beta) \\
m^2_{\tilde{e}_R} &= m_0^2 + 0.15 m^2_{1/2} - 0.23 M_Z^2 \cos(2\beta)
\end{aligned} \tag{B7}$$

In the case of the third generation sparticles, left– and right–handed sfermions will mix; for a given sfermion $\tilde{f} = \tilde{t}, \tilde{b}$ and $\tilde{\tau}$, the mass matrices which determine the mixing are

$$\left[\begin{array}{cc} m^2_{\tilde{f}_L} + m_f^2 & m_f(A_f - \mu r_f) \\ m_f(A_f - \mu r_f) & m^2_{\tilde{f}_R} + m_f^2 \end{array} \right] \tag{B8}$$

where the sfermion masses $m_{\tilde{f}_{L,R}}$ are given above, m_f are the masses of the partner fermions and $r_b = r_\tau = 1/r_t = \tan\beta$. These matrices are diagonalized by orthogonal matrices with mixing angles θ_f defined by

$$\sin 2\theta_f = \frac{2 m_f (A_f - \mu r_f)}{m^2_{\tilde{f}_1} - m^2_{\tilde{f}_2}} \quad , \quad \cos 2\theta_f = \frac{m^2_{\tilde{f}_L} - m^2_{\tilde{f}_R}}{m^2_{\tilde{f}_1} - m^2_{\tilde{f}_2}} \tag{B9}$$

and the masses of the squark eigenstates given by

$$m^2_{\tilde{f}_{1,2}} = m_f^2 + \frac{1}{2} \left[m^2_{\tilde{f}_L} + m^2_{\tilde{f}_R} \mp \sqrt{(m^2_{\tilde{f}_L} - m^2_{\tilde{f}_R})^2 + 4 m_f^2 (A_f - \mu r_f)^2} \right] . \tag{B10}$$

Appendix C: Renormalization Group Equations

Finally, we collect for completeness the renormalization group equations for the soft–SUSY breaking parameters [the trilinear couplings, scalar masses as well as for μ and B], including the dependence on A_t, A_b and A_τ. We restrict ourselves to the one–loop RGE's and we keep only the leading terms in the mass hierarchy in the MSSM with three fermion generations. The complete expressions for the RGE's can be found in Refs.[13, 19].

For the trilinear couplings of the third generation sfermions, the RGE's are given by

$$\begin{aligned}
\frac{dA_t}{dt} &= \frac{2}{16\pi^2} \Big(\sum c_i g_i^2 M_i + 6\lambda_t^2 A_t + \lambda_b^2 A_b \Big) \\
\frac{dA_b}{dt} &= \frac{2}{16\pi^2} \Big(\sum c'_i g_i^2 M_i + 6\lambda_b^2 A_b + \lambda_t^2 A_t + \lambda_\tau^2 A_\tau \Big) \\
\frac{dA_\tau}{dt} &= \frac{2}{16\pi^2} \Big(\sum c''_i g_i^2 M_i + 3\lambda_b^2 A_b + 4\lambda_\tau^2 A_\tau \Big)
\end{aligned} \tag{C1}$$

while for the scalar masses of the third generation sfermions, one has

$$
\begin{aligned}
\frac{dM^2_{Q_L}}{dt} &= \frac{2}{16\pi^2}\Big(-\frac{1}{15}g_1^2M_1^2 - 3g_2^2M_2^2 - \frac{16}{3}g_3^2M_3^2 + \lambda_t^2X_t + \lambda_b^2X_b\Big) \\
\frac{dM^2_{t_R}}{dt} &= \frac{2}{16\pi^2}\Big(-\frac{16}{15}g_1^2M_1^2 - \frac{16}{3}g_3^2M_3^2 + 2\lambda_t^2X_t\Big) \\
\frac{dM^2_{b_R}}{dt} &= \frac{2}{16\pi^2}\Big(-\frac{4}{15}g_1^2M_1^2 - \frac{16}{3}g_3^2M_3^2 + 2\lambda_b^2X_b\Big) \\
\frac{dM^2_{L_L}}{dt} &= \frac{2}{16\pi^2}\Big(-\frac{3}{5}g_1^2M_1^2 - 3g_2^2M_2^2 + \lambda_\tau^2X_\tau\Big) \\
\frac{dM^2_{\tau_R}}{dt} &= \frac{2}{16\pi^2}\Big(-\frac{12}{5}g_1^2M_1^2 + 2\lambda_\tau^2X_\tau\Big)
\end{aligned}
\tag{C2}
$$

The evolution parameter is defined by $t = \log(Q/M_G)$,

$$
\begin{aligned}
b_i &= (\,33/5\,,\,1\,,\,-3\,) \\
c_i &= (\,13/15\,,\,3\,,\,16/3\,) \\
c'_i &= (\,7/15\,,\,3\,,\,16/3\,) \\
c''_i &= (\,9/5\,,\,3\,,\,0\,)
\end{aligned}
\tag{C3}
$$

and

$$
\begin{aligned}
X_t &= M^2_{Q_L} + M^2_{t_R} + M^2_{H_2} + A_t^2 \\
X_b &= M^2_{Q_L} + M^2_{b_R} + M^2_{H_1} + A_b^2 \\
X_\tau &= M^2_{L_L} + M^2_{\tau_R} + M^2_{H_1} + A_\tau^2
\end{aligned}
\tag{C4}
$$

For the first and second generation sfermions, these expressions reduce to

$$
\begin{aligned}
\frac{dA_u}{dt} &= \frac{2}{16\pi^2}\Big(\sum c_i g_i^2 M_i + \lambda_t^2 A_t\Big) \\
\frac{dA_d}{dt} &= \frac{2}{16\pi^2}\Big(\sum c'_i g_i^2 M_i + \lambda_b^2 A_b + \frac{1}{3}\lambda_\tau^2 A_\tau\Big) \\
\frac{dA_e}{dt} &= \frac{2}{16\pi^2}\Big(\sum c''_i g_i^2 M_i + \lambda_b^2 A_b + \frac{1}{3}\lambda_\tau^2 A_\tau\Big)
\end{aligned}
\tag{C5}
$$

and

$$
\begin{aligned}
\frac{dM^2_{q_L}}{dt} &= \frac{2}{16\pi^2}\Big(-\frac{1}{15}g_1^2M_1^2 - 3g_2^2M_2^2 - \frac{16}{3}g_3^2M_3^2\Big) \\
\frac{dM^2_{u_R}}{dt} &= \frac{2}{16\pi^2}\Big(-\frac{16}{15}g_1^2M_1^2 - \frac{16}{3}g_3^2M_3^2\Big) \\
\frac{dM^2_{d_R}}{dt} &= \frac{2}{16\pi^2}\Big(-\frac{4}{15}g_1^2M_1^2 - \frac{16}{3}g_3^2M_3^2\Big) \\
\frac{dM^2_{l_L}}{dt} &= \frac{2}{16\pi^2}\Big(-\frac{3}{5}g_1^2M_1^2 - 3g_2^2M_2^2\Big) \\
\frac{dM^2_{e_R}}{dt} &= \frac{2}{16\pi^2}\Big(-\frac{12}{5}g_1^2M_1^2\Big)
\end{aligned}
\tag{C6}
$$

For the gauge coupling constants and the other soft–SUSY breaking parameters, the RGE's are given by

$$\frac{dg_i}{dt} = \frac{1}{16\pi^2} b_i g_i^3 \tag{C7}$$

$$\frac{dM_i}{dt} = \frac{2}{16\pi^2} b_i g_i^2 M_i \tag{C8}$$

$$\frac{dB}{dt} = \frac{2}{16\pi^2}\Big(\frac{3}{5}g_1^2 M_1 + 3g_2^2 M_2 + 3\lambda_b^2 A_b + 3\lambda_t^2 A_t + \lambda_\tau^2 A_\tau\Big) \tag{C9}$$

$$\frac{d\mu}{dt} = \frac{\mu}{16\pi^2}\Big(-\frac{3}{5}g_1^2 - 3g_2^2 + 3\lambda_t^2 + 3\lambda_b^2 + \lambda_\tau^2\Big) \tag{C10}$$

$$\frac{dm_{H_1}^2}{dt} = \frac{2}{16\pi^2}\Big(-\frac{3}{5}g_1^2 M_1^2 - 3g_2^2 M_2^2 + 3\lambda_b^2 X_b + \lambda_\tau^2 X_\tau\Big) \tag{C11}$$

$$\frac{dm_{H_2}^2}{dt} = \frac{2}{16\pi^2}\Big(-\frac{3}{5}g_1^2 M_1^2 - 3g_2^2 M_2^2 + 3\lambda_t^2 X_t\Big) \tag{C12}$$

References

[1] J. Wess and B. Zumino, Phys. Lett. B49 (1974) 52.

[2] For reviews on supersymmetric theories, see P. Fayet and S. Ferarra, Phys. Rep. 32 (1977) 249; H. P. Nilles, Phys. Rep. 110 (1984) 1. R. Barbieri, Riv. Nuovo Cimento 11 (1988) 1; H. Haber and G. Kane, Phys. Rep. 117 (1985) 75.

[3] P. W. Higgs, Phys. Rev. Lett. 12 (1964) 132 and Phys. Rev. 145 (1966) 1156; F. Englert and R. Brout, Phys. Rev. Lett. 13 (1964) 321; G. S. Guralnik, C. R. Hagen and T. W. Kibble, Phys. Rev. Lett. 13 (1964) 585.

[4] For a review on the Higgs sector in the MSSM, see J.F. Gunion, H.E. Haber, G. Kane and S. Dawson, The Higgs Hunter's Guide, Addison–Wesley, Reading 1990.

[5] H. Georgi, H. Quinn and S. Weinberg, Phys. Rev. Lett. 33 (1974) 451.

[6] J. Ellis, S. Kelley and D. V. Nanopoulos, Phys. Lett. 260B (1991) 131; U. Amaldi, W. de Boer and H. Fürstenau, Phys. Lett. 260B (1991) 447; P. Langacker and M. Luo, Phys. Rev. D44 (1991) 817; G. G. Ross and R. G. Roberts, Nucl. Phys. B377 (1992) 571.

[7] The LEP Electroweak Working Group, Report CERN–PPE/95–172.

[8] K. Inoue, A. Kakuto, H. Komatsu and S. Takeshita, Prog. Theor. Phys. **68** (1982) 927; **71** (1984) 413; L. E. Ibañez and G. G. Ross, Phys. Lett. **B110** (1982) 215; L. Alvarez-Gaumé, M. Claudson and M. B. Wise, Nucl. Phys. **B207** (1982) 96; J. Ellis, D. V. Nanopoulos, and K. Tamvakis, Phys. Lett. **B121** (1983) 123; M. Drees, Phys. Rev. **D38** (1988) 718.

[9] J. Ellis, L. Fogli and M. Lisi, Z. Phys. **C69** (1996) 627; P. Chankowski and S. Pokorski, Phys. Lett. *B356* (1995) 307.

[10] M. Veltman, Nucl. Phys. **B123** (1977) 89.

[11] M. Chanowitz, J. Ellis and M. Gaillard, Nucl. Phys. 128 (1977) 506.

[12] B. Pendleton and G. G. Ross, Phys. Lett. **98B** (1981) 291; C. T. Hill, Phys. Rev. **D24** (1981) 691.

[13] V. Barger, M.S. Berger, and P. Ohmann, Phys. Rev. **D47**, (1993) 1093.

[14] V. Barger, M.S. Berger, P. Ohmann, and R.J.N. Phillips, Phys. Lett. **B314** (1993) 351; M. Carena, S. Pokorski, and C. E. M. Wagner, Nucl. Phys. **B406** (1993) 59.

[15] F. Abe et al., CDF Coll., Phys. Rev. Lett. **74** (1995) 2626; S. Abachi et al., DO Coll., Phys. Rev. Lett. **74** (1995) 2632; F. Abe et al., CDF Coll., FNAL–PUB–96/004.

[16] H.E. Haber, Report CERN–TH/95–109, Proceedings *Conference on Beyond the Standard Model IV*, Lake Tahoe CA 1994; World Sci., J.F. Gunion et al., eds.

[17] Y. Okada, M. Yamaguchi and T. Yanagida, Prog. Theor. Phys. **85** (1991) 1; H.E. Haber and R. Hempfling, Phys. Rev. Lett. **66** (1991) 1815; J. Ellis, G. Ridolfi and F. Zwirner, Phys. Lett. **257B** (1991) 83; R. Barbieri, F. Caravaglios and M. Frigeni, Phys. Lett. **258B** (1991) 167.

[18] H.E. Haber and G. Kane in Ref.[2].

[19] V. Barger, M. S. Berger, and P. Ohmann, Phys. Rev. **D49**, (1994) 4908.

[20] W. de Boer et al., IEKP-KA/96-04, hep-ph/9603350.

[21] F. M. Borzumati, M. Olechowski, and S. Pokorski, Phys. Lett. **B349**, 311 (1995); H. Murayama, M. Olechowski, and S. Pokorski, UCB-PTH-95/34, hep-ph/9510327.

[22] M. Drees and M. Nojiri, Nucl. Phys. **B369** (1992) 54.

[23] S. Bethke, Proceedings of the *QCD 1994*, Montpellier 1994.

[24] J.-F. Grivaz, Proc. *Europhysics Conference on High Energy Physics*, Brussels 1995; for the recent limits including LEP1.5 data, see: D. Buskulic et al., Aleph Collab. CERN–PPE–96–010; G. Alexander et al., OPAL Collab. CERN–PPE–019, 020; M. Acciarri et al., L3 Collab. CERN–PPE–96–029.

[25] J. Ellis, G. Ridolfi, and F. Zwirner, Phys. Lett. **B262**, 477 (1991); A. Brignole, J. Ellis, G. Ridolfi, and F. Zwirner, Phys. Lett. **B271**, 123 (1991).

[26] M. Drees, Phys. Lett. **B181**, (1986) 279; J. S. Hagelin and S. Kelley, Nucl. Phys. **B342**, (1990) 95.

[27] A. Djouadi, G. Girardi, W. Hollik, F. Renard and C. Verzegnassi, Nucl. Phys. **B349** (1991) 48; M. Boulware and D. Finnell, Phys. Rev. **D44** (1991) 2054.

[28] See for instance W. Hollik, Proc. *Europhysics Conference on High Energy Physics*, Brussels 1995; J. D. Wells, C. Kolda, and G. L. Kane Phys. Lett. **B338** (1994) 219.

[29] G. Kane, C. Kolda, L. Roszkowski, and J. D. Wells, Phys. Rev. **D49**, (1994) 6173.

[30] A. J. Buras, M. Misiak, M. Münz, and S. Pokorski, Nucl. Phys. **B424**, (1994) 374.

[31] V. Barger, M. S. Berger, P. Ohmann and R. J. N. Phillips, Phys. Rev. **D51**, (1995) 2438; B. de Carlos and J. A. Casas, Phys. Lett. **B349**, (1995) 300, erratum – *ibid.* **351**, (1995) 604.

[32] A. Djouadi, J. Kalinowski and P. M. Zerwas, Z. Phys. **C57**, (1993) 569.

[33] A. Djouadi, J. Kalinowski and P. M. Zerwas, Z. Phys. **C70** (1996) 435.

[34] A. Djouadi, M. Spira and P. M. Zerwas, Z. Phys. **C70** (1996) 427.

[35] J.F. Gunion and H.E. Haber, Nucl. Phys. **B272** (1986) 1; **B278** (1986) 449; **B307** (1988) 445; erratum hep-ph/9301201.

[36] A. Bartl et al., Phys. Lett. **B373** (1996) 117.

[37] J.F. Gunion and H.E. Haber, Phys. Rev. **D37** (1988) 2515.

[38] M. El Kheishen, A. Shafik and A. Aboshousha, Phys. Rev. **D45** (1992) 4345.

[39] L. E. Ibañez and and C. Lopez, Nucl. Phys. **B233** (1984) 511.

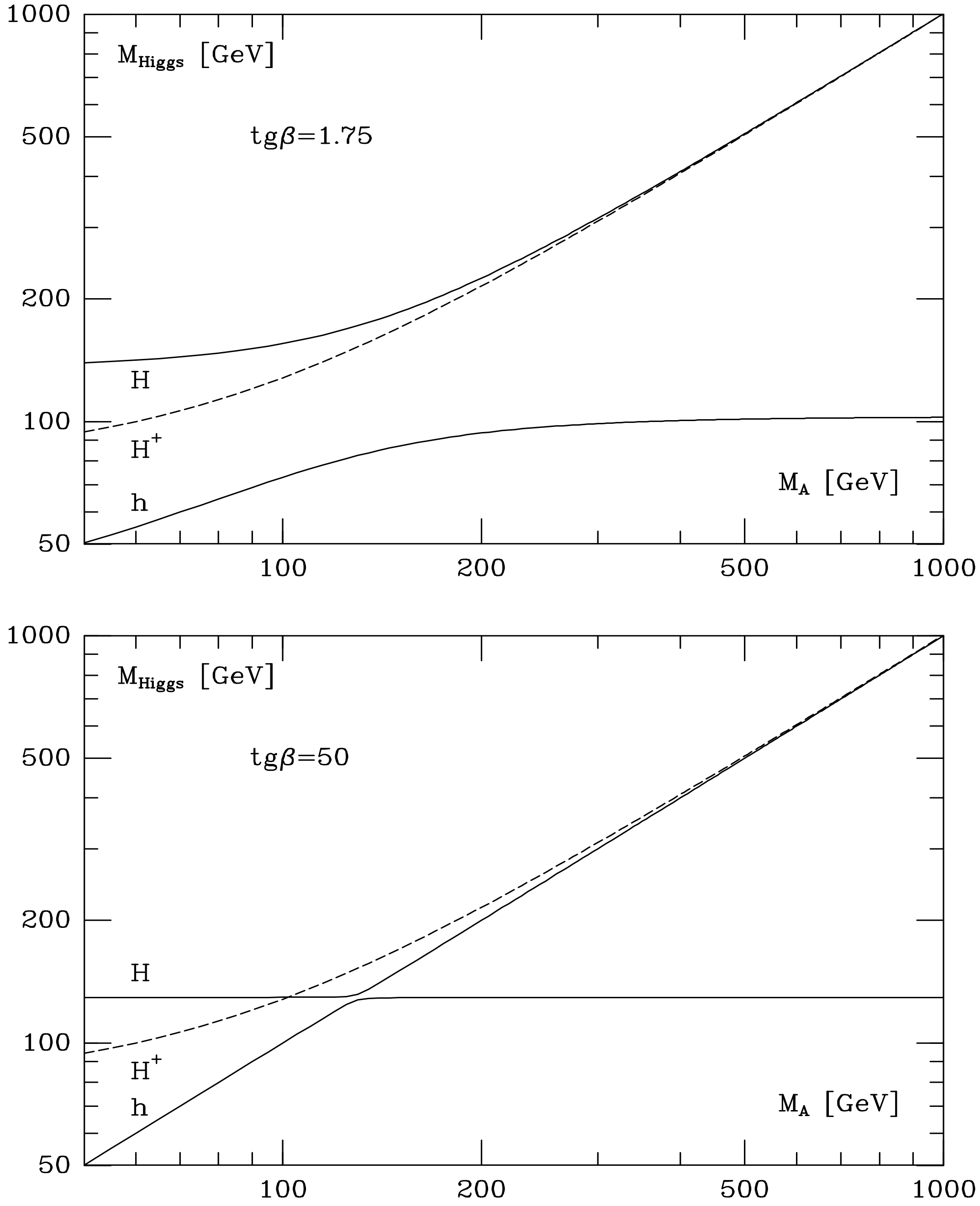

Fig. 1: Masses of the CP–even Higgs bosons h, H and of the charged Higgs particles $H^{\pm}$ as a function of M_A for two values of $\tan\beta = 1.75$ and 50; the common squark mass M_S at the weak scale is fixed to $M_S = 1$ TeV and we take $\mu = A_t = 0$.

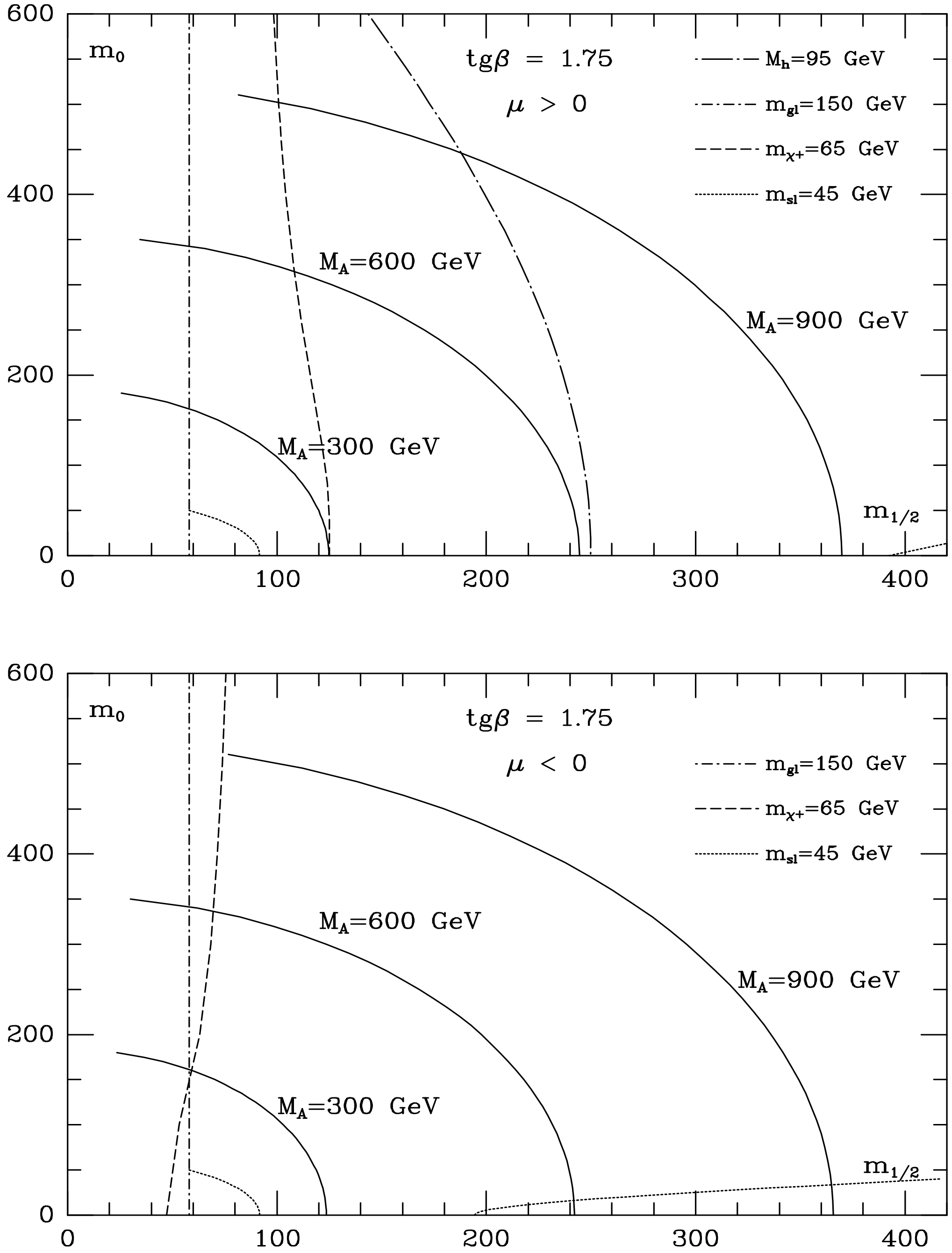

Fig. 2: The correlation between m_0 and $m_{1/2}$ for $\tan\beta = 1.75$ and three values of $M_A = 300, 600$ and 900 GeV. The non-solid lines show the boundaries which can be excluded by including the experimental bounds from LEP1.5 and Tevatron.

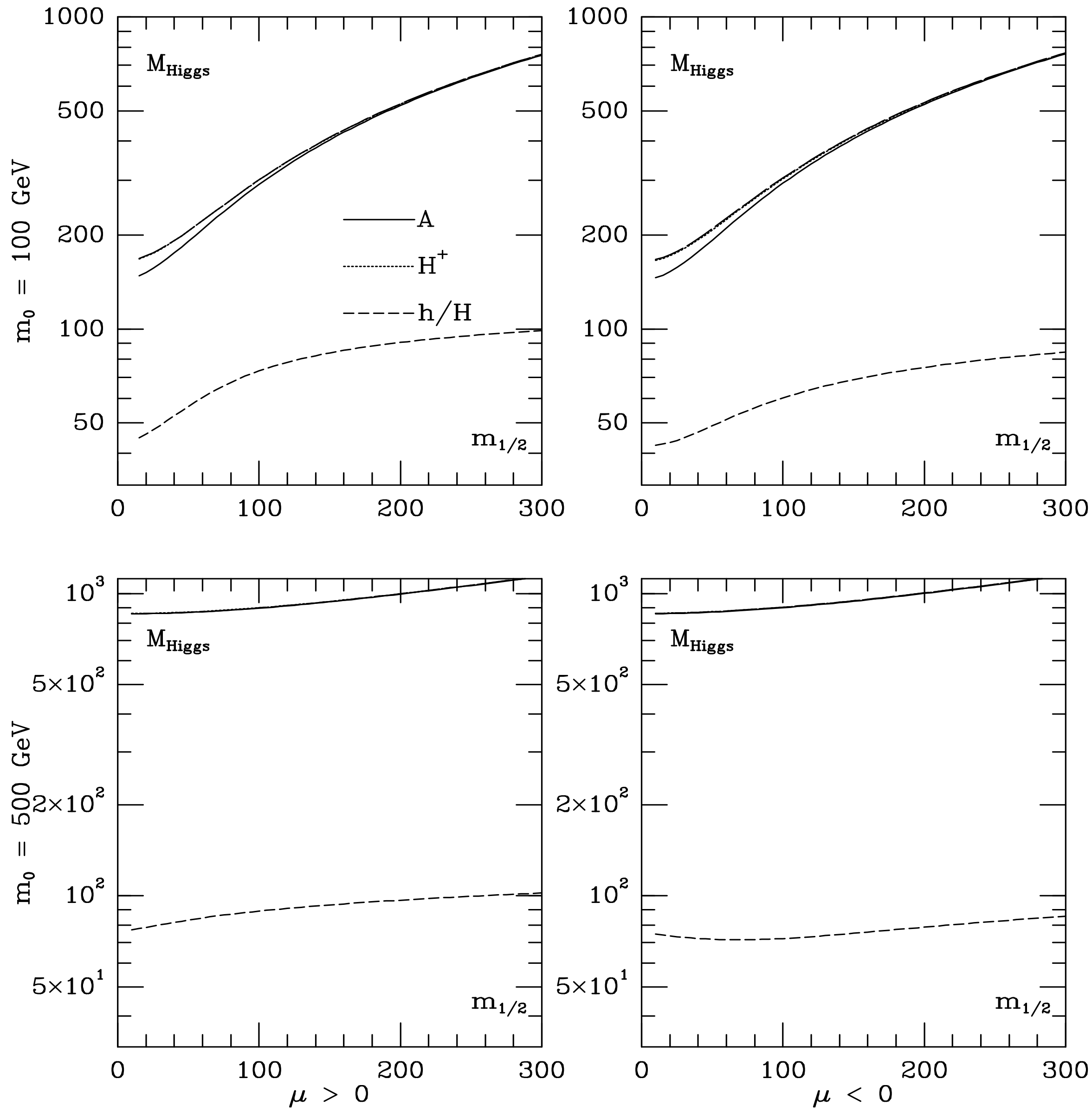

Fig. 3a: The masses of the Higgs bosons as a function of $m_{1/2}$ for $\tan\beta = 1.75$, for the two values $m_0 = 100$ and 500 GeV and both signs of μ.

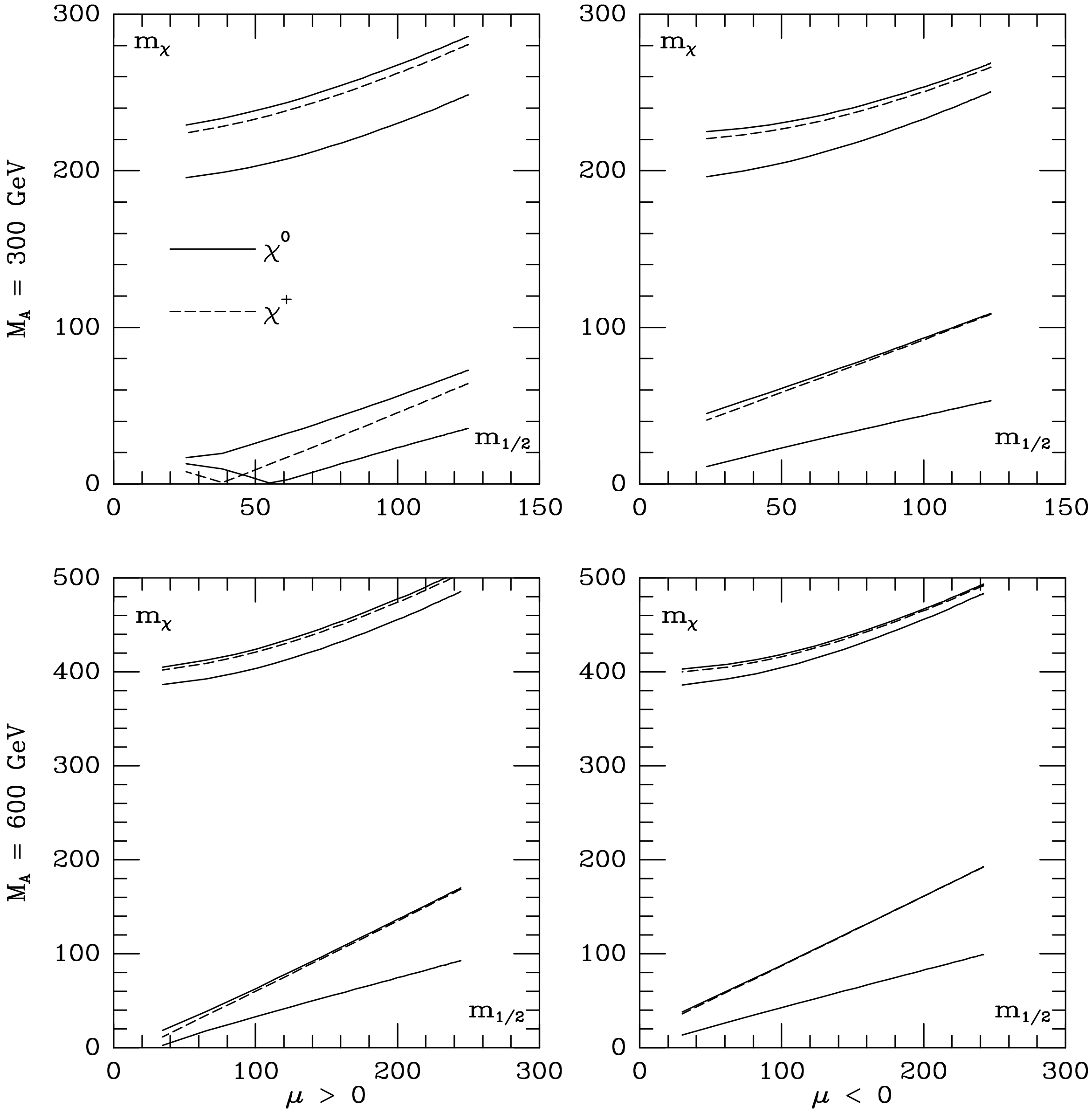

Fig. 3b: The masses of the two charginos (dashed lines) and the four neutralinos (solid lines) as a function of $m_{1/2}$ for $\tan\beta = 1.75$, $M_A = 300$ and 600 GeV and for both signs of μ. The chargins/neutralinos are ordered with increasing masses.

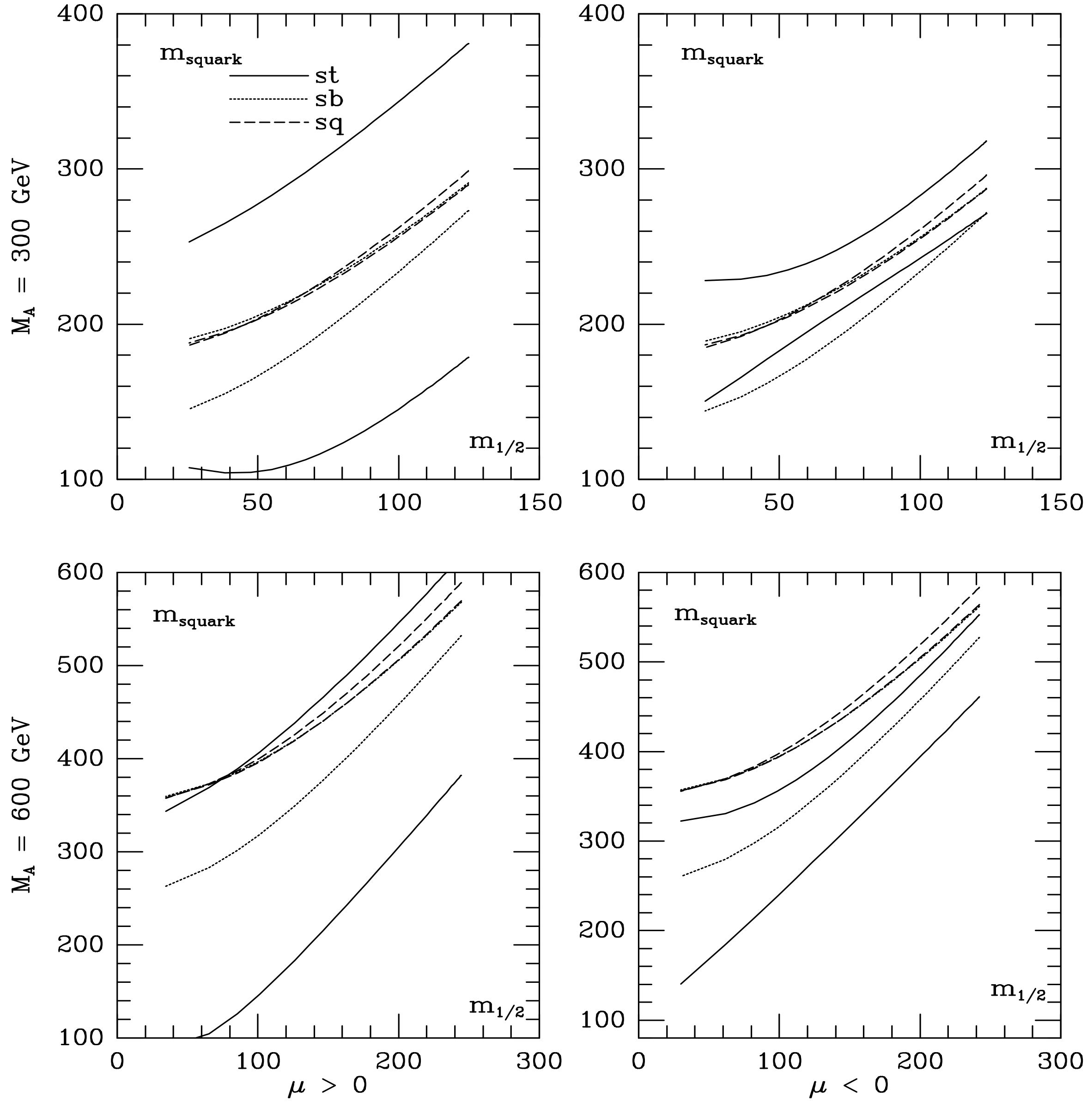

Fig. 3c: The masses of the two stop (solid lines), sbottom (dotted lines) and first/second generation squark (dashed lines) eigenstates as a function of $m_{1/2}$ for $\tan\beta = 1.75$, $M_A = 300$ and 600 GeV and for both signs of μ.

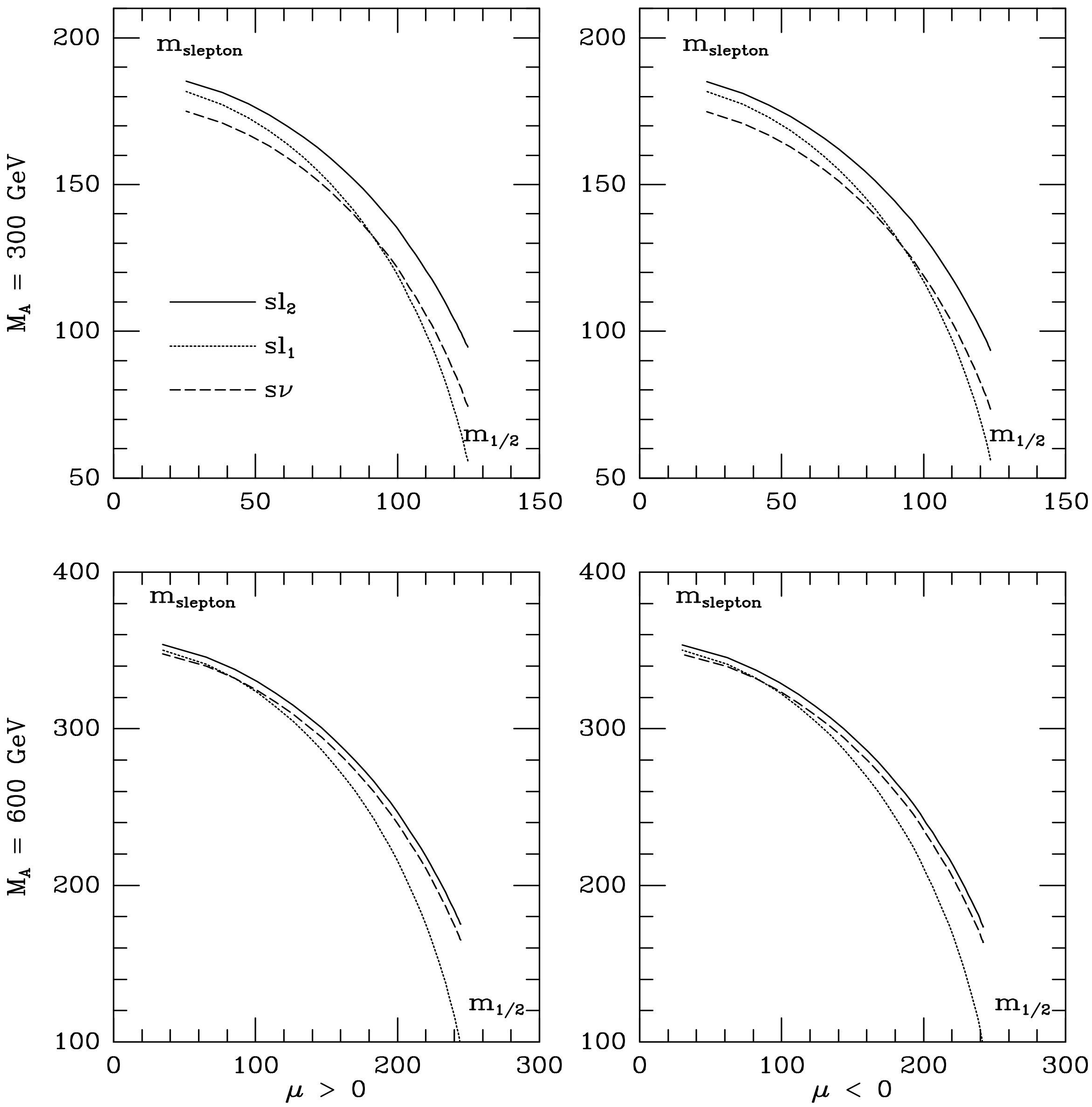

Fig. 3d: The masses of the charged sleptons (solid and dotted lines) and the sneutrino (dashed lines) of the three generations as a function of $m_{1/2}$ for $\tan\beta = 1.75$, $M_A = 300$ and 600 GeV and for both signs of μ.

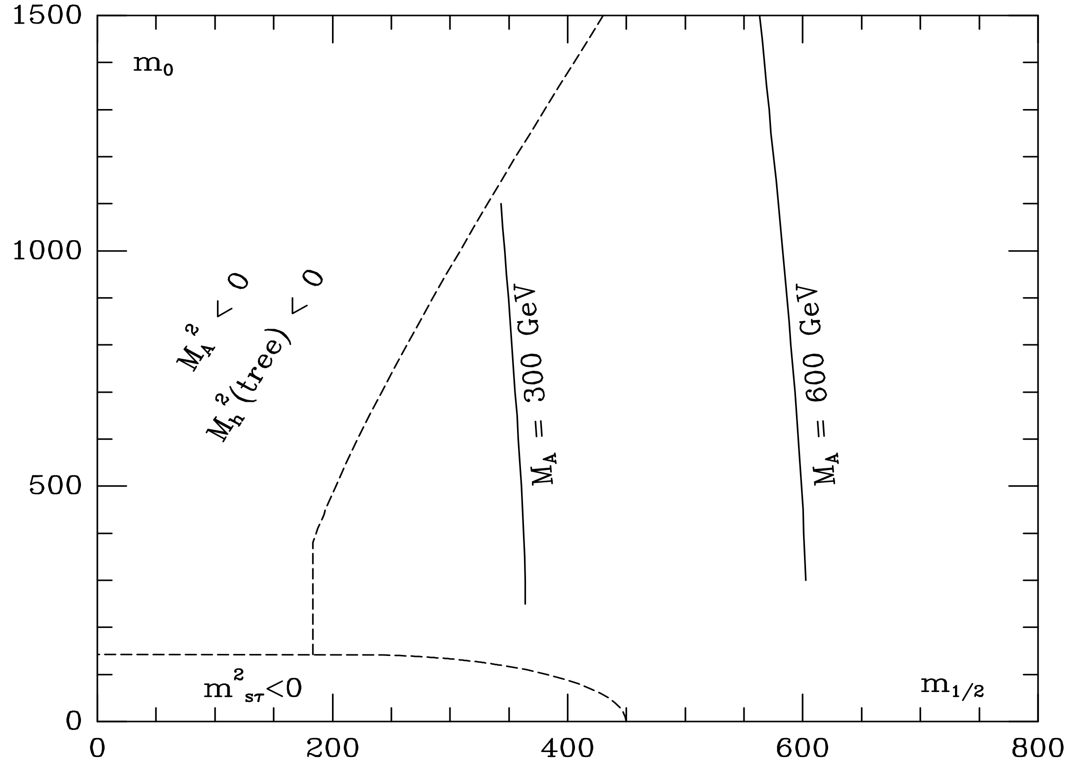

Fig. 4: The correlation between m_0 and $m_{1/2}$ for $\tan\beta \simeq 50$, $\mu < 0$, and two values of $M_A = 300$ and 600 GeV. The boundary contours correspond to tachyonic solutions, $m^2_{\tilde{\tau}} < 0$, $M_A^2 < 0$ and $M_h^2 < 0$ at the tree–level.

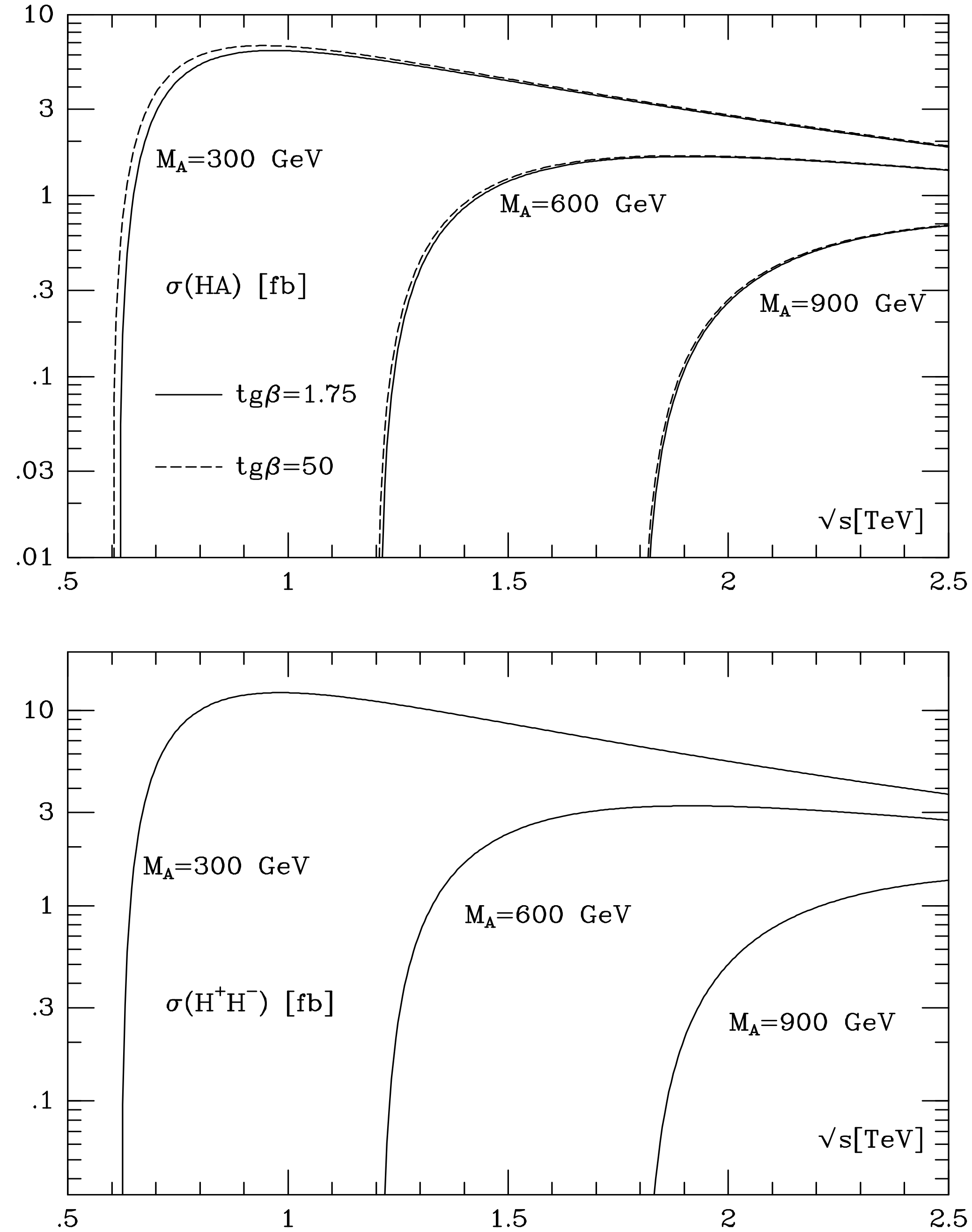

Fig. 5a: Cross sections for the pair production processes $e^+e^- \to HA$ and $e^+e^- \to H^+H^-$ as a function of $\sqrt{s}$ for $\tan\beta = 1.75$ (solid lines) and $\tan\beta = 50$ (dashed lines) and three values of $M_A = 300, 600$ and 900 GeV.

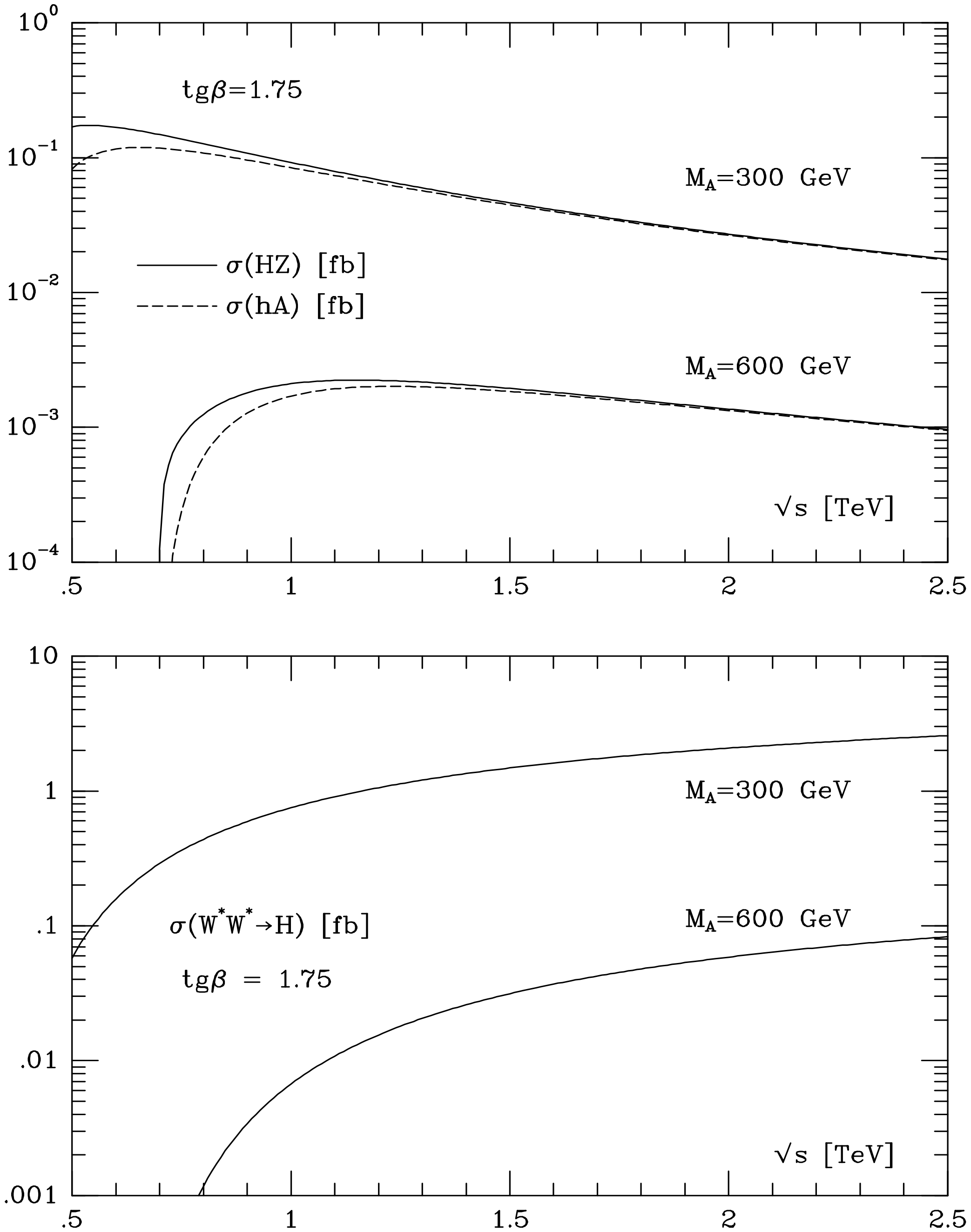

Fig. 5b: Cross sections for the production processes $e^+e^- \to HZ$, $e^+e^- \to hA$ and $e^+e^- \to H\nu\bar{\nu}$ as a function of $\sqrt{s}$ for $\tan\beta = 1.75$ and the values $M_A = 300$ and 600 GeV.

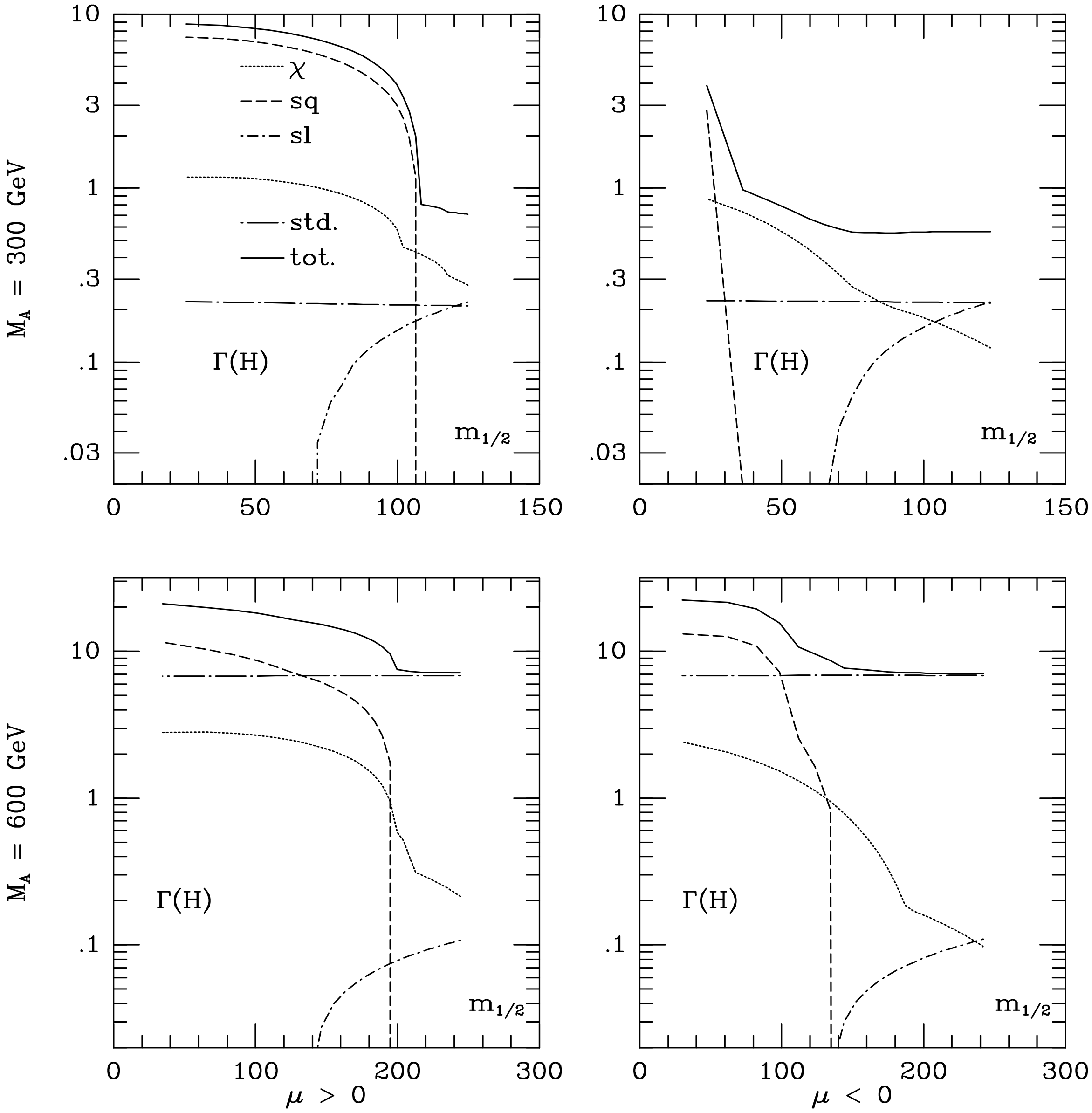

Fig. 6a: Decay widths (in GeV) of the heavy CP–even Higgs boson H into charginos and neutralinos (dotted lines), squarks (dashed lines), sleptons (dash–dotted lines), standard particles (dott–long–dashed lines) and the total decay widths (solid lines) as a function of $m_{1/2}$ for $\tan\beta = 1.75$, $M_A = 300$ and 600 GeV and for both signs of μ.

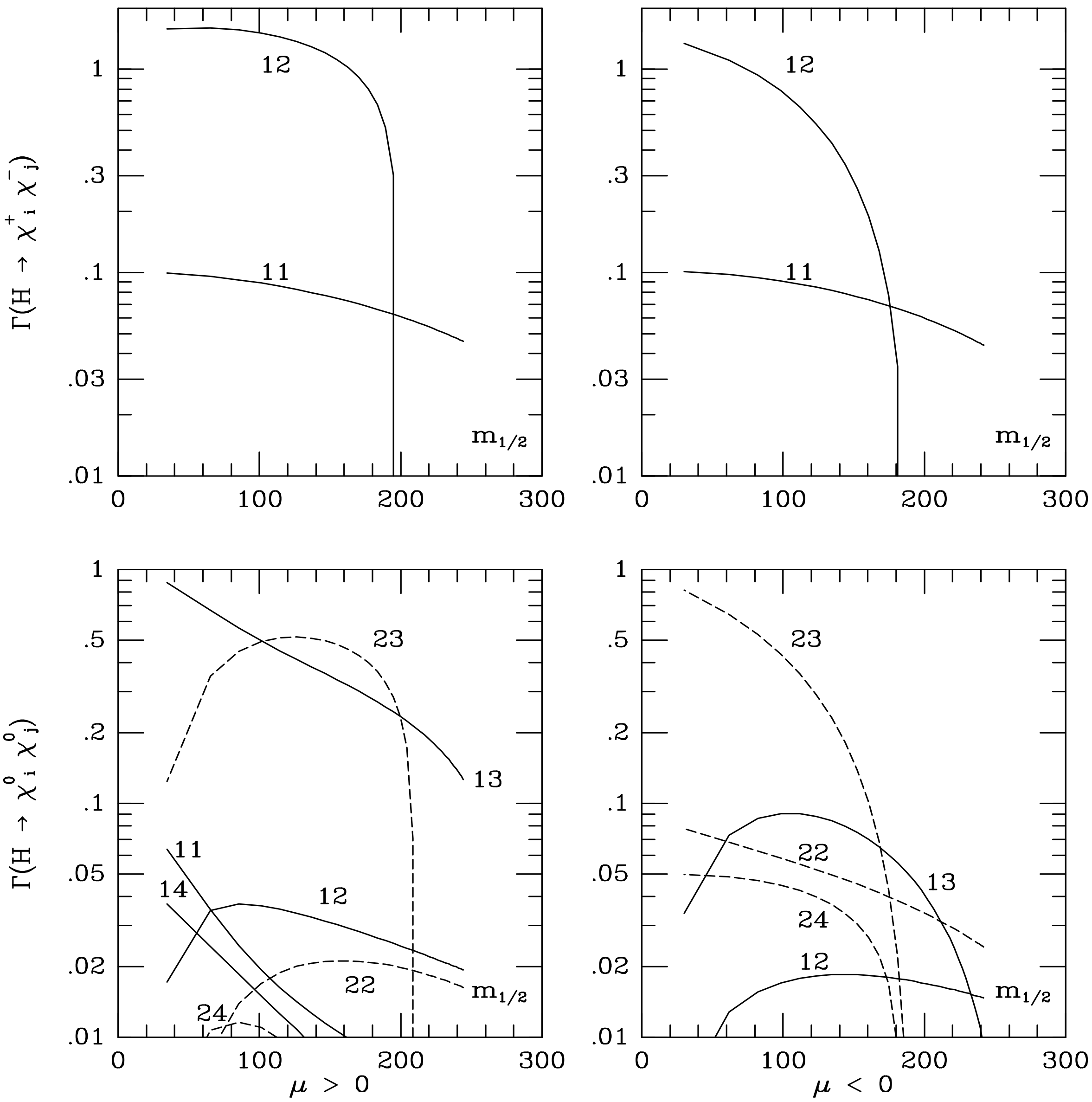

Fig. 6b: Partial decay widths (in GeV) of the heavy CP–even Higgs boson H into all combinations of chargino and neutralino pairs $[ij \equiv \chi_i \chi_j]$ as a function of $m_{1/2}$ for $\tan\beta = 1.75$, $M_A = 600$ GeV and for both signs of μ.

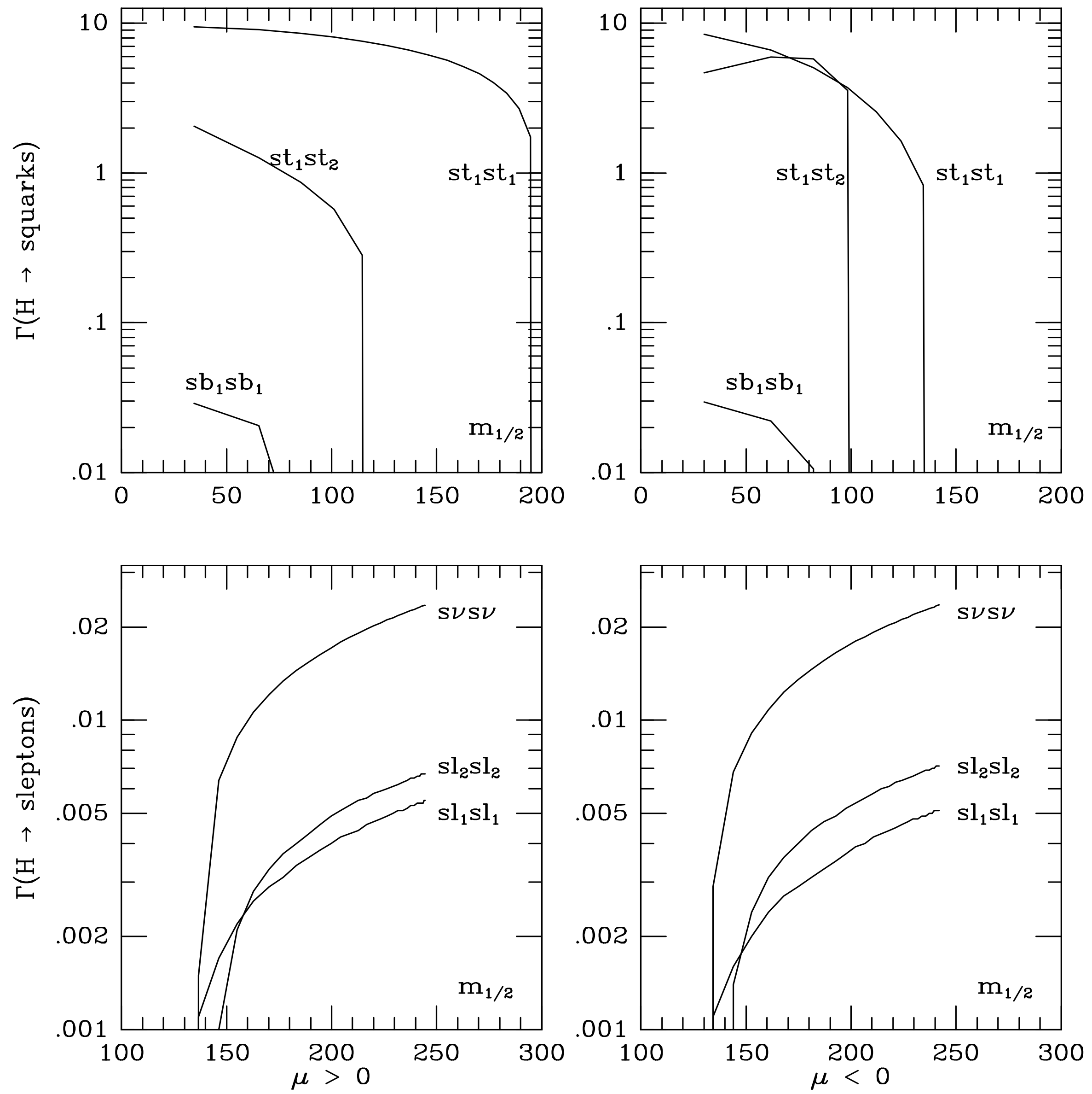

Fig. 6c: Partial decay widths (in GeV) of the heavy CP–even Higgs boson H into stop and sbottom squarks and into slepton pairs as a function of $m_{1/2}$ for $\tan\beta = 1.75$, $M_A = 600$ GeV and for both signs of μ.

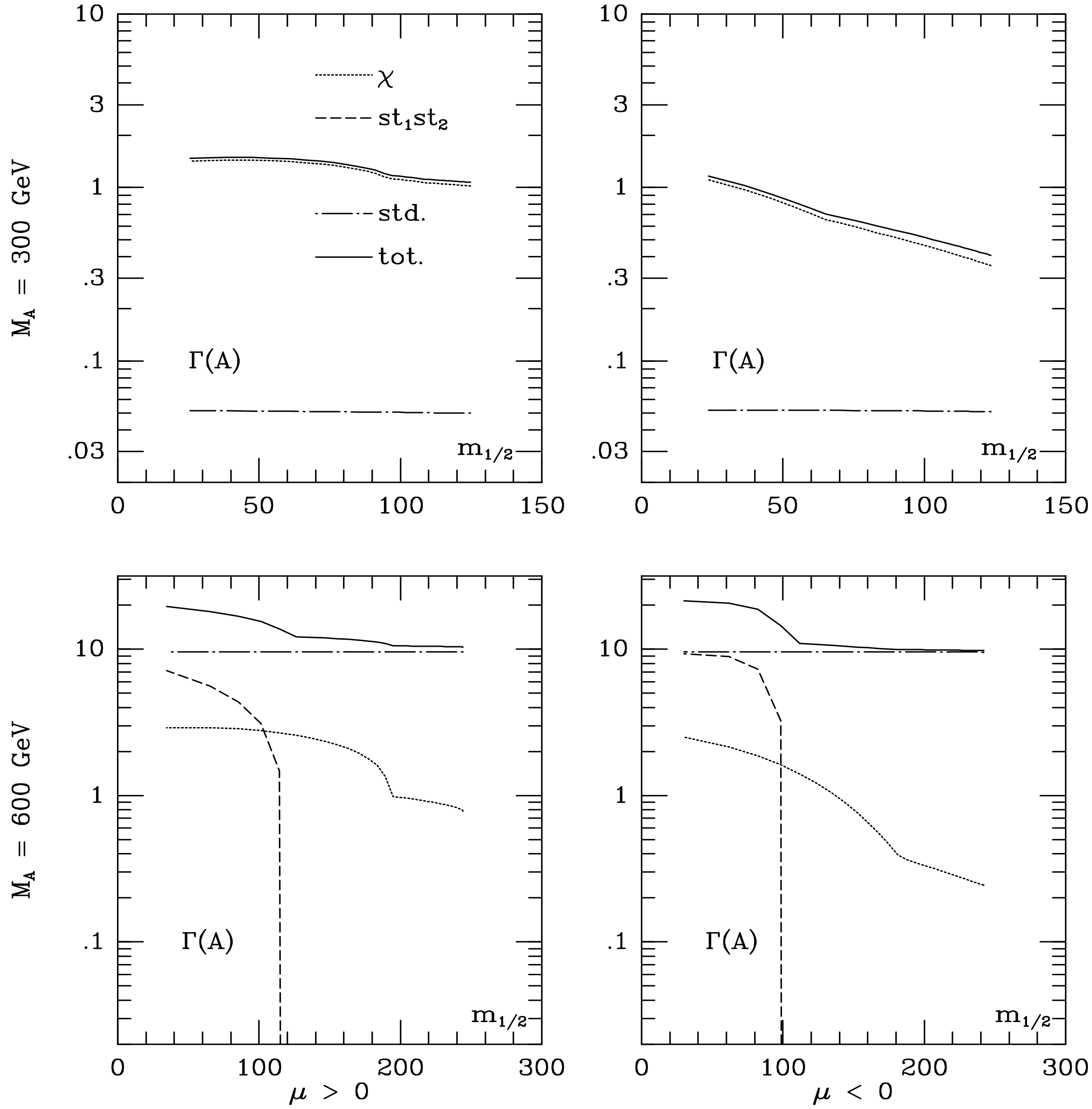

Fig. 7a: Decay widths (in GeV) of the pseudoscalar Higgs boson A into charginos and neutralinos (dotted lines), stop squarks (dashed lines), standard particles (dott–long–dashed lines) and the total decay widths (solid lines) as a function of $m_{1/2}$ for $\tan\beta = 1.75$, $M_A = 300$ and 600 GeV and for both signs of μ.

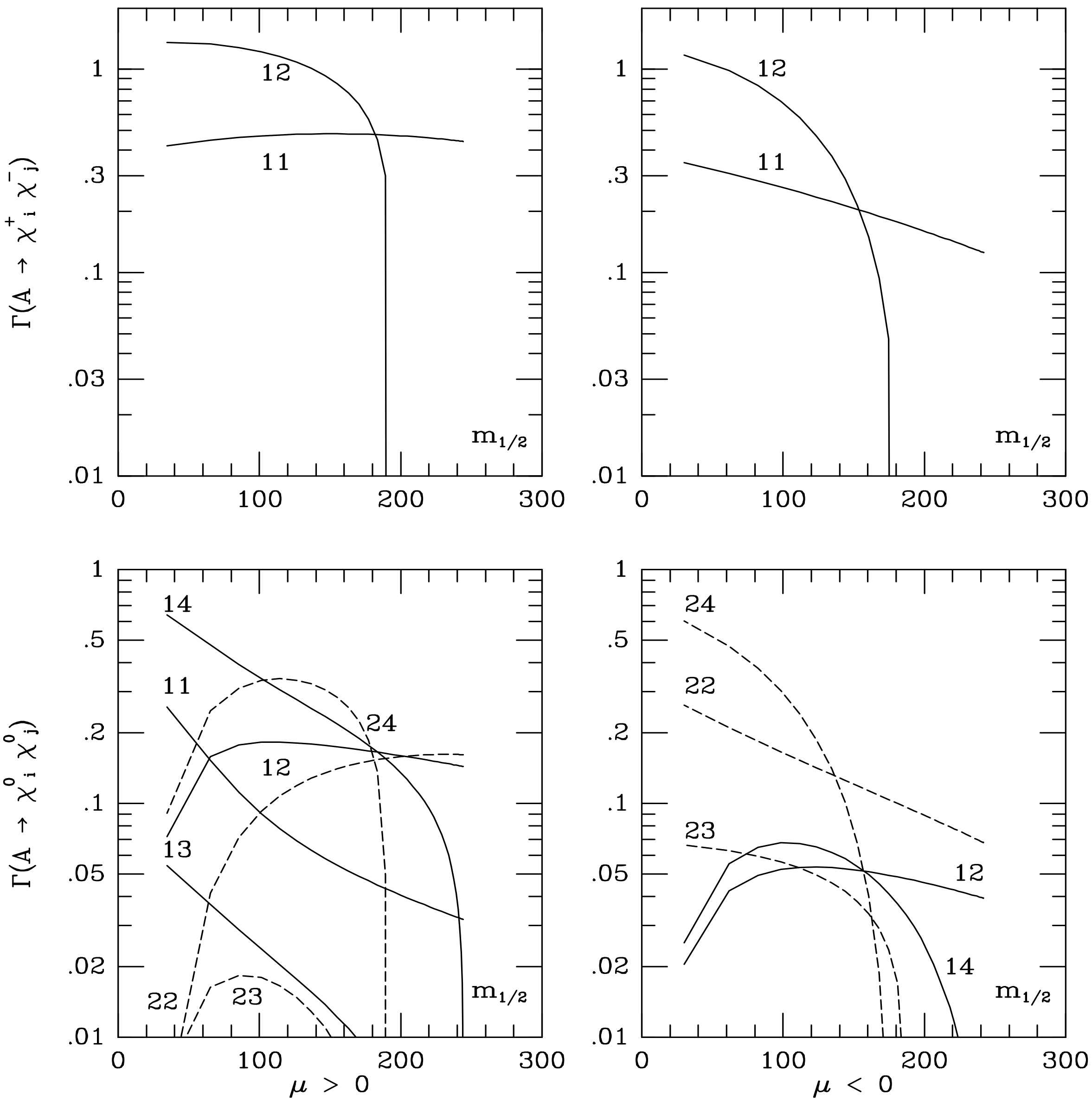

Fig. 7b: Partial decay widths (in GeV) of the pseudoscalar Higgs boson A into all combinations of chargino and neutralino pairs $[ij \equiv \chi_i \chi_j]$ as a function of $m_{1/2}$ for $\tan\beta = 1.75$, $M_A = 600$ GeV and for both signs of μ.

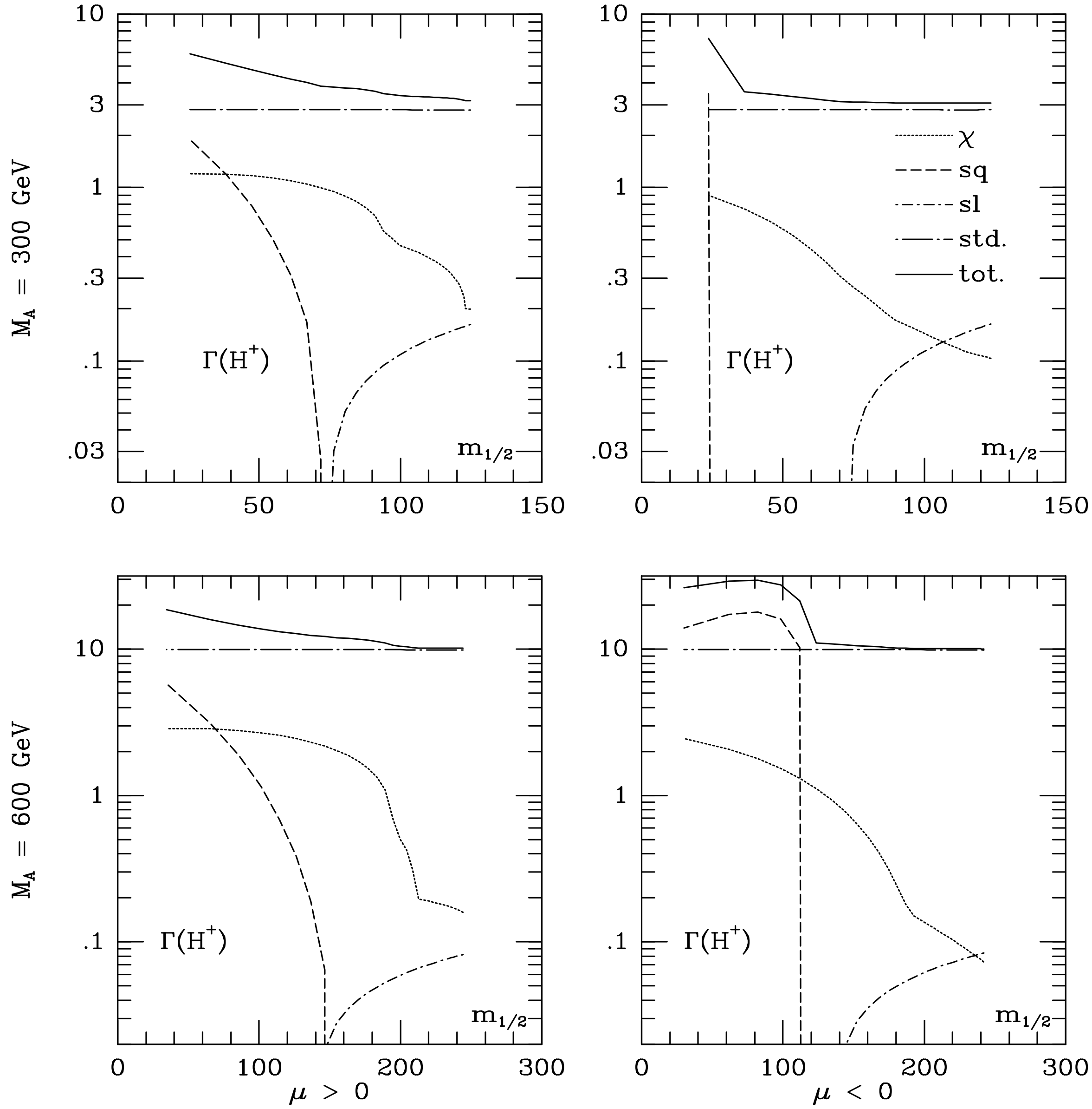

Fig. 8a: Decay widths (in GeV) of the charged Higgs bosons into charginos and neutralinos (dotted lines), squarks (dashed lines), sleptons (dash–dotted lines), standard particles (dott–long–dashed lines) and the total decay widths (solid lines) as a function of $m_{1/2}$ for $\tan\beta = 1.75$, $M_A = 300$ and 600 GeV and for both signs of μ.

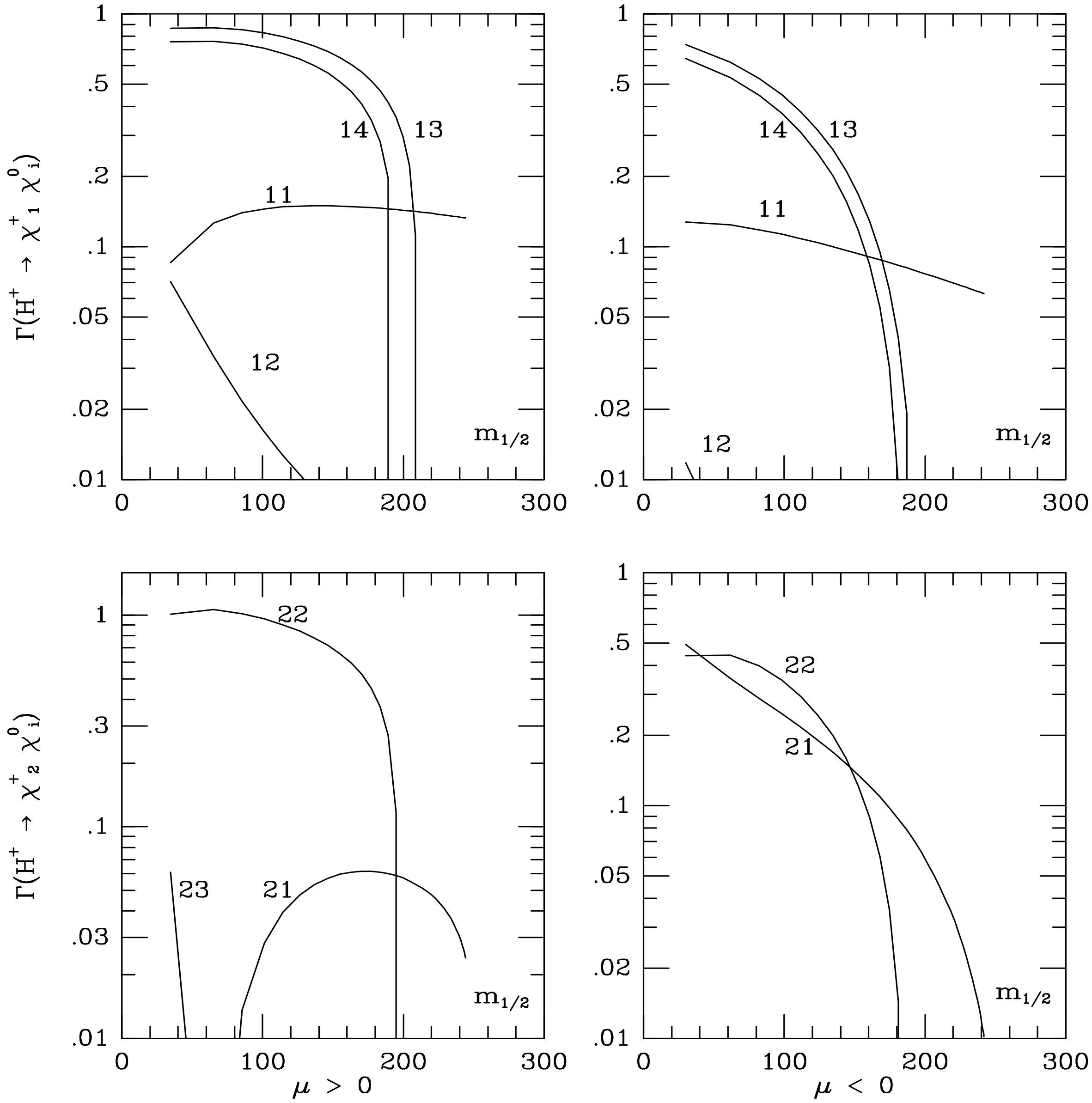

Fig. 8b: Partial decay widths (in GeV) of the charged Higgs boson $H^{\pm}$ into all combinations of charginos and neutralinos $[ij \equiv \chi_i^+ \chi_j^0]$ as a function of $m_{1/2}$ for $\tan\beta = 1.75$, $M_A = 600$ GeV and for both signs of μ.